DGCR8 Mediates Repair of UV-Induced DNA Damage Independently of RNA Processing

Calses, Philamer C. ; Dhillon, Kiranjit K. ; Tucker, Nyka ; Chi, Yong ; Huang, Jen-wei ; Kawasumi, Masaoki ; Nghiem, Paul ; Wang, Yemin ;…

(Citation)
Cell Reports,19(1):162-174

(Issue Date)
2017-04-04

(Resource Type)
journal article

(Version)
Version of Record

(URL)
https://hdl.handle.net/20.500.14094/90004317

Article

Cell Reports

DGCR8 Mediates Repair of UV-Induced DNA Damage Independently of RNA Processing

Graphical Abstract

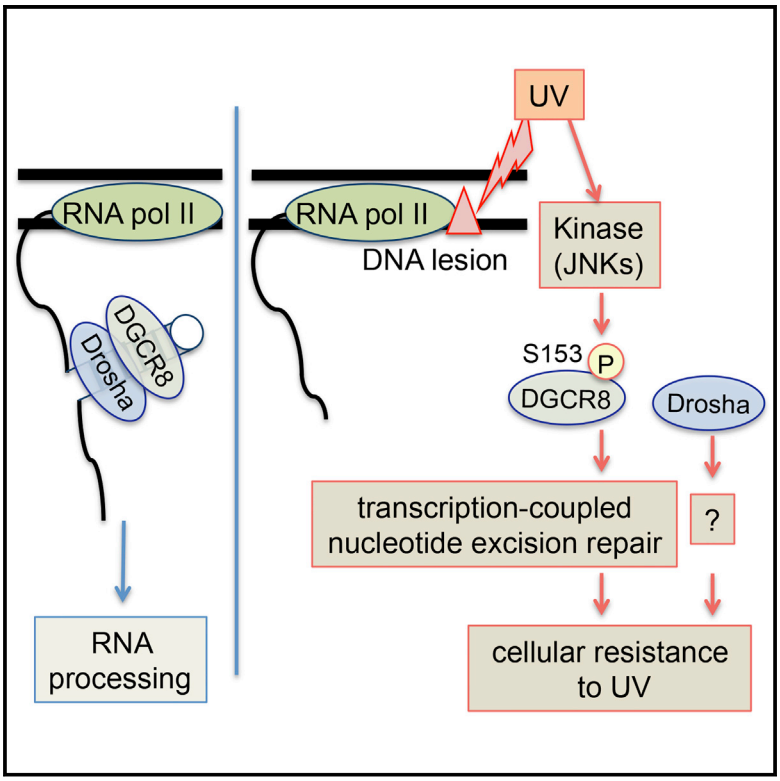

Authors

Philamer C. Calses, Kiranjit K. Dhillon, Nyka Tucker, ..., Kaoru Sugasawa, Masafumi Saijo, Toshiyasu Taniguchi

Correspondence

ttaniguc@fhcrc.org

In Brief

Calses et al. find that UV-induced phosphorylation on serine 153 of DGCR8, an RNA binding protein involved in microRNA processing, is critical for cellular resistance to UV through DNA repair of UV-induced lesions.

Highlights

- UV radiation induces phosphorylation on S153 of DGCR8
- Phosphorylation on S153 of DGCR8 mediates cellular resistance to UV
- S153 phosphorylation mediates transcription-coupled nucleotide excision repair
- JNKs are involved in UV-induced phosphorylation of S153 of DGCR8

Calses et al., 2017, Cell Reports *19*, 162–174
April 4, 2017
http://dx.doi.org/10.1016/j.celrep.2017.03.021

OPEN ACCESS
CellPress

Cell Reports
Article

DGCR8 Mediates Repair of UV-Induced DNA Damage Independently of RNA Processing

Philamer C. Calses,[1,2,4] Kiranjit K. Dhillon,[1,2] Nyka Tucker,[1,2] Yong Chi,[1,3] Jen-wei Huang,[1,2,4] Masaoki Kawasumi,[5] Paul Nghiem,[5] Yemin Wang,[1,2] Bruce E. Clurman,[1,3] Celine Jacquemont,[1,2] Philip R. Gafken,[6] Kaoru Sugasawa,[7] Masafumi Saijo,[8] and Toshiyasu Taniguchi[1,2,9,10,*]

[1]Division of Human Biology
[2]Division of Public Health Sciences
[3]Division of Clinical Research
Fred Hutchinson Cancer Research Center, 1100 Fairview Ave. N., C1-015, Seattle, WA 98109-1024, USA
[4]Molecular and Cellular Biology Graduate Program, University of Washington, 1959 NE Pacific, HSB T-466, Seattle, WA 98195-7275, USA
[5]Division of Dermatology, Department of Medicine, University of Washington, 850 Republican St., Seattle, WA 98109-4714, USA
[6]Proteomics Core Facility, Fred Hutchinson Cancer Research Center, 1100 Fairview Ave. N., DE-352, Seattle, WA 98109-1024, USA
[7]Biosignal Research Center, Organization of Advanced Science and Technology, Kobe University, 1-1 Rokkodai-cho, Nada-ku, Kobe, Hyogo 657-8501, Japan
[8]Graduate School of Frontier Biosciences, Osaka University, Yamadaoka 1-3, Suita, Osaka 565-0871, Japan
[9]Department of Molecular Life Science, Tokai University School of Medicine, 143 Shimokasuya, Isehara, Kanagawa 259-1193, Japan
[10]Lead Contact
*Correspondence: ttaniguc@fhcrc.org
http://dx.doi.org/10.1016/j.celrep.2017.03.021

SUMMARY

Ultraviolet (UV) radiation is a carcinogen that generates DNA lesions. Here, we demonstrate an unexpected role for DGCR8, an RNA binding protein that canonically functions with Drosha to mediate microRNA processing, in the repair of UV-induced DNA lesions. Treatment with UV induced phosphorylation on serine 153 (S153) of DGCR8 in both human and murine cells. S153 phosphorylation was critical for cellular resistance to UV, the removal of UV-induced DNA lesions, and the recovery of RNA synthesis after UV exposure but not for microRNA expression. The RNA-binding and Drosha-binding activities of DGCR8 were not critical for UV resistance. DGCR8 depletion was epistatic to defects in XPA, CSA, and CSB for UV sensitivity. DGCR8 physically interacted with CSB and RNA polymerase II. JNKs were involved in the UV-induced S153 phosphorylation. These findings suggest that UV-induced S153 phosphorylation mediates transcription-coupled nucleotide excision repair of UV-induced DNA lesions in a manner independent of microRNA processing.

INTRODUCTION

UV irradiation generates DNA photoproducts, mainly cyclobutane pyrimidine dimers (CPDs) and 6-4 photoproducts (6-4PPs), and causes cell cycle arrest, apoptosis, mutagenesis, and proliferative transformation (Herrlich et al., 2008). These DNA lesions are repaired by nucleotide excision repair (NER) in mammalian cells (Hanawalt and Spivak, 2008). Deficiencies in NER are associated with human genetic disorders such as xeroderma pigmentosum (XP), Cockayne syndrome (CS), cerebro-oculo-facio-skeletal syndrome (COFS), UV-sensitive syndrome (UVSS), and trichothiodystrophy (TTD). The NER pathway operates through two subpathways: global genome NER(GG-NER) and transcription-coupled NER (TC-NER). In GG-NER, XPC and UV-DDB recognize damage sites throughout the genome, whereas TC-NER is initiated by RNA polymerase II (RNAPII), which is blocked by DNA lesions during transcription. These subpathways converge on a common downstream pathway to resolve the DNA lesions (Hanawalt and Spivak, 2008).

DGCR8 is a critical protein for microRNA (miRNA) biogenesis (Macias et al., 2013). miRNAs are small, single-stranded, noncoding RNAs that post-transcriptionally regulate gene expression (Carthew and Sontheimer, 2009) and have been implicated in many biological processes, including DNA damage response and repair (Wang and Taniguchi, 2013), and in the pathogenesis of many human diseases (Iorio and Croce, 2012). miRNAs are initially transcribed as long primary miRNAs (pri-miRNAs) (Carthew and Sontheimer, 2009). Pri-miRNAs are processed by the microprocessor complex, consisting of Drosha (an RNase III-type enzyme) and DGCR8, a double-stranded RNA-binding protein, to generate ~70-nt precursor miRNAs (pre-miRNAs) (Carthew and Sontheimer, 2009). Pre-miRNAs are exported to the cytoplasm, where they are cleaved by another RNase III, Dicer, to generate ~22-nt mature miRNA duplexes. Apart from its critical role in miRNA biogenesis, DGCR8 also regulates the stability of some mRNAs and small nucleolar RNAs (snoRNAs) (Macias et al., 2012, 2013). The two double-stranded RNA (dsRNA)-binding domains of DGCR8 are required for recognition of the RNA substrates (Macias et al., 2012; Sohn et al., 2007; Yeom et al., 2006).

DGCR8 is regulated in several ways. MeCP2 binds to the dsRNA-binding domains of DGCR8 and prevents the binding

of Drosha to DGCR8 (Cheng et al., 2014). A heme group promotes the dimerization of DGCR8 and facilitates miRNA processing (Weitz et al., 2014). Deacetylation of DGCR8 also enhances miRNA processing (Wada et al., 2012). DGCR8 is phosphorylated at 23 sites, and these modifications increase DGCR8 protein stability (Herbert et al., 2013). Some of the 23 phosphorylation sites may be targets of ERK/mitogen-activated protein kinase (MAPK) (Herbert et al., 2013), but there are likely other kinases involved as well.

miRNAs have been implicated in the cellular response to UV radiation: the expression of a subset of miRNAs is altered in response to UV radiation (Dziunycz et al., 2010; Pothof et al., 2009), and depletion of factors required for miRNA biogenesis leads to cellular sensitivity to UV (Pothof et al., 2009). However, the mechanisms connecting the miRNA biogenesis machinery and UV response remain unclear, and whether UV sensitivity of miRNA biogenesis protein-deficient cells is mediated by the miRNA biogenesis defect is not clear.

Here, we show an unexpected function of DGCR8 in the repair of UV-induced DNA lesions that is independent of miRNA processing.

RESULTS

DGCR8 Is Phosphorylated in Response to UV Radiation

Initially, we found that DGCR8 was phosphorylated in response to UV radiation by performing a western blot analysis of ultraviolet C (UV-C)-treated human and murine cells (Figures 1A and 1B). We subsequently performed mass spectrometry of DGCR8 protein immunopurified from UV-C-irradiated human HeLa cells and identified nine phosphorylation sites (S95, S153, S271, S275, T371, S373, S377, S434, and S619) (Figure 1C; Figures S1A and S1B). Site-directed mutagenesis experiments for each of these sites revealed that S153 was phosphorylated in a UV-induced manner (Figure 1E). S153 of DGCR8 is conserved among mammals but not in other vertebrates (Figure 1D; Figure S1C).

Next we generated a phospho-specific antibody using a peptide that flanks S153 of human DGCR8 as an immunogen (Figure 1D). The specificity of the antibody was confirmed using S153A mutant cells and phosphatase treatment (Figure 1E; Figure S1D). S153 phosphorylation was detected in untreated cells and was increased in response to UV radiation in a time- and dose-dependent manner (Figure 1F) in multiple human cell lines, including primary fibroblasts and keratinocytes (Figure 1G). S153 phosphorylation was also induced by treatment with ultraviolet B (UV-B), a chemical UV mimetic (4-nitroquinoline-1-oxide [4-NQO]), and oxidizers, including hydrogen peroxide and potassium bromate, but not with other DNA-damaging agents and cellular stresses we have tested (Figure 1H; Figure S1E). We also generated a phospho-specific antibody using a peptide that flanks S153 of murine Dgcr8 as an immunogen (Figure 1D) and confirmed UV-induced phosphorylation of S153 in mouse embryonic fibroblasts (MEFs) (Figure S1F). Subcellular fractionation experiments revealed that S153-phosphorylated DGCR8 was detected in the nuclear soluble and chromatin fractions (Figure S1G). The S153 phosphorylation signal was induced diffusely in the nucleus (Figure S1H), even after localized UV irradiation through a micropore filter (Figure S1I), indicating that the distribution of S153-phosphorylated DGCR8 is not limited to sites of UV-induced DNA lesions. Furthermore, almost all of the UV-irradiated cells showed increased phosphorylation of S153 (Figures S1H and S1I), suggesting that the UV-induced S153 phosphorylation occurs in a cell cycle-independent manner.

DGCR8 Phosphorylation Mediates Cellular Resistance to UV Radiation

To test the functional significance of UV-induced phosphorylation of S153, we examined the UV sensitivity of DGCR8-deficient cells. Depletion of DGCR8 in a human colorectal cancer cell line (HCT-116) using three independent short hairpin RNAs (shRNAs) resulted in hypersensitivity to UV-C and UV-B (Figure 2A; Figure S2A). We also recapitulated the UV-C sensitivity phenotype with DGCR8 depletion in human fibroblasts (Figure 4B; Figure S4C). Reintroduction of shRNA-resistant wild-type DGCR8 or an S153D phospho-mimetic mutant into DGCR8-depleted HCT116 cells restored UV-C resistance. However, the S153A phospho-mutant failed to restore UV-C or UV-B resistance (Figures 2B and 2C; Figure S2A), suggesting that S153 phosphorylation is critical for cellular resistance to UV. Similarly, DGCR8-depleted cells were hypersensitive to hydrogen peroxide, and complementation with wild-type or S153D DGCR8 restored resistance to hydrogen peroxide whereas the S153A mutant did not (Figure S2B). Dgcr8 knockout MEFs were sensitive to UV-C and UV-B compared with Dgcr8 knockout MEFs transduced with wild-type human DGCR8 or wild-type mouse Dgcr8, whereas Dgcr8 knockout MEFs transduced with S153A mutant human DGCR8 or S153A mutant mouse Dgcr8 were as sensitive to UV as Dgcr8 knockout MEFs (Figures S2C and S2D).

Previous studies have shown that mutations introduced into two dsRNA-binding domains of DGCR8 abolish miRNA processing activity (Yeom et al., 2006). Surprisingly, complementation of DGCR8-depleted cells with the dsRNA binding domain mutants (mDRBD1/2) restored UV-C and UV-B resistance (Figures 2B and 2C; Figure S2A), indicating that the RNA binding activity and miRNA processing functions of DGCR8 are not required for UV resistance.

Among the various DGCR8 deletion mutants we tested (Figure 2B; Figure S2E), the Δ692 (Drosha-binding deficient) mutant (Yeom et al., 2006) restored UV-C resistance in DGCR8-depleted cells (Figure 2C), whereas other mutants with large deletions (Δ275, Δ483, and Δ276–773) (Yeom et al., 2006) failed to do so (Figure S2F). In contrast, the Δ692 S153A mutant failed to restore UV resistance in DGCR8-depleted cells (Figure 2C). The Δ692 or Δ692 S153A mutant proteins were not co-immunoprecipitated with Drosha as expected, whereas wild-type DGCR8 and the DGCR8 S153A mutant were co-immunoprecipitated with Drosha (Figure 2D). Altogether, these findings indicate that S153 phosphorylation is critical for UV resistance whereas the DGCR8-Drosha interaction is not.

Interestingly, Drosha depletion also led to hypersensitivity to UV-C and UV-B, which was rescued by reintroduction of wild-type Drosha and the ΔC114 (miRNA processing-deficient) or ΔN490 (miRNA processing-deficient and DGCR8

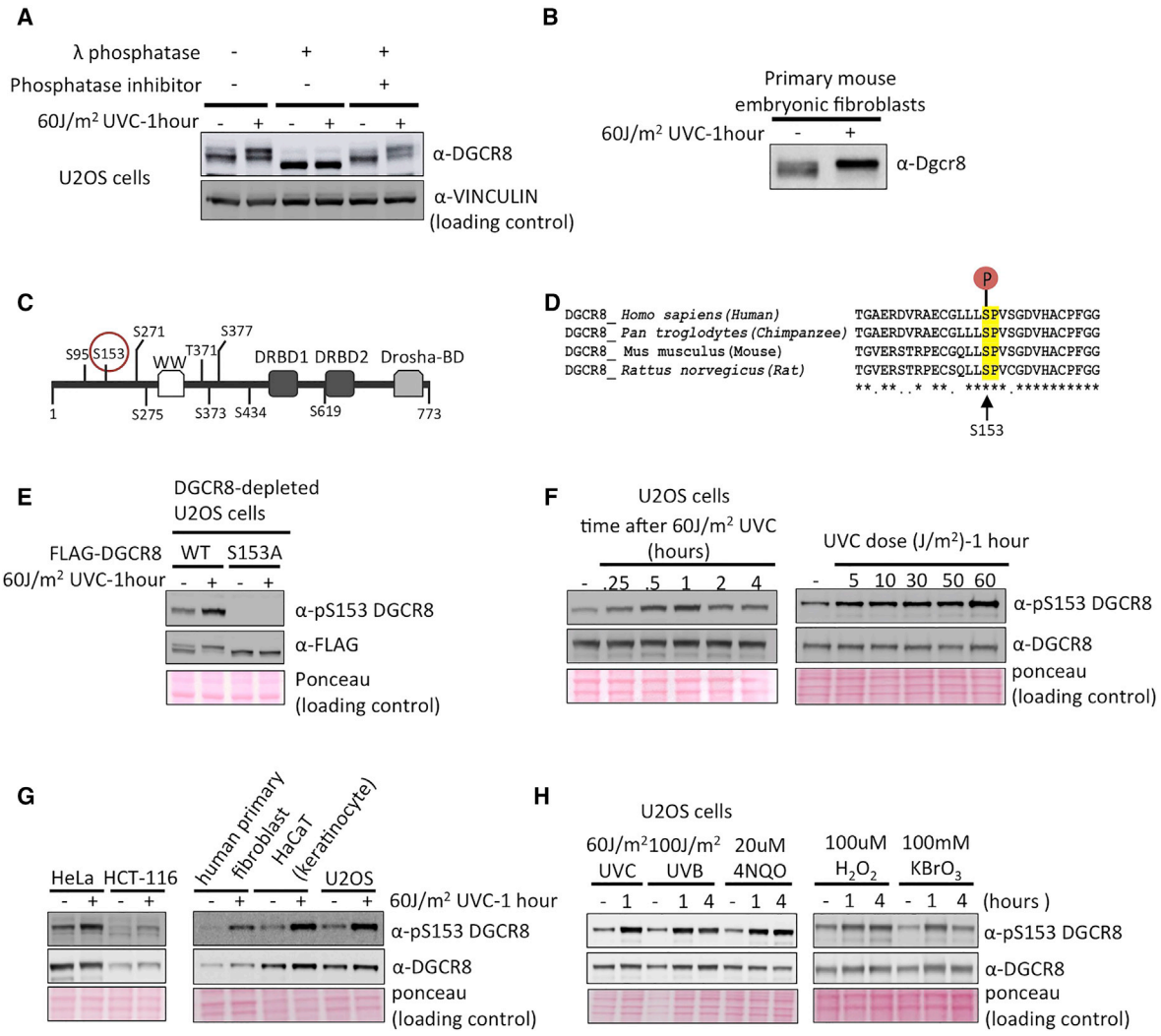

Figure 1. S153 of DGCR8 Is Phosphorylated in Response to UV Radiation

(A) Immunoblot. Cell lysates from U2OS cells treated with UV-C were treated with λ phosphatase and phosphatase inhibitors and immunoblotted for DGCR8 and vinculin (loading control).

(B) Cell lysates from primary murine embryonic fibroblasts were immunoblotted for Dgcr8.

Large gels were used for the western blots shown in (A) and (B) to clearly see the shift of the bands.

(C) Schematic of nine phosphorylation sites of human DGCR8 identified by mass spectrometry (not proportional to actual size). The DGCR8 protein contains a WW domain, two dsRNA binding domains (DRBD1 and DRBD2), and a Drosha binding domain (Drosha-BD).

(D) Sequence alignment of S153 surrounding amino acids. S153 is conserved among mammals.

(E) Immunoblot. U2OS cells depleted of DGCR8 and transfected with shRNA-resistant FLAG-WT DGCR8 or FLAG-S153A DGCR8, UV-irradiated or not, were immunoblotted for DGCR8 or FLAG.

(F–H) Immunoblots. The indicated cells were irradiated with UV or not and harvested at the indicated time points or treated with other agents continuously as indicated. (F) Time course and dose dependency experiments after UV-C treatment. (G) Various cell lines were tested after UV-C exposure. (H) Response to various agents was tested.

See also Figure S1.

binding-deficient) Drosha mutants (Han et al., 2004; Figures 3A and 3B; Figure S2G). These data suggest that the DGCR8 binding or the miRNA processing activities of Drosha are not required for UV resistance. Furthermore, UV-induced phosphorylation of S153 on DGCR8 occurred normally in Drosha-depleted cells (Figure 3C). These findings collectively suggest that DGCR8 and Drosha are independently required for UV resistance and that the miRNA processing activity of the Drosha-DGCR8 microprocessor complex is not required for UV resistance.

DGCR8 Phosphorylation Does Not Alter miRNA Expression

Next, to determine whether S153 on DGCR8 is critical for miRNA expression, we conducted miRNA profiling using qRT-PCR of

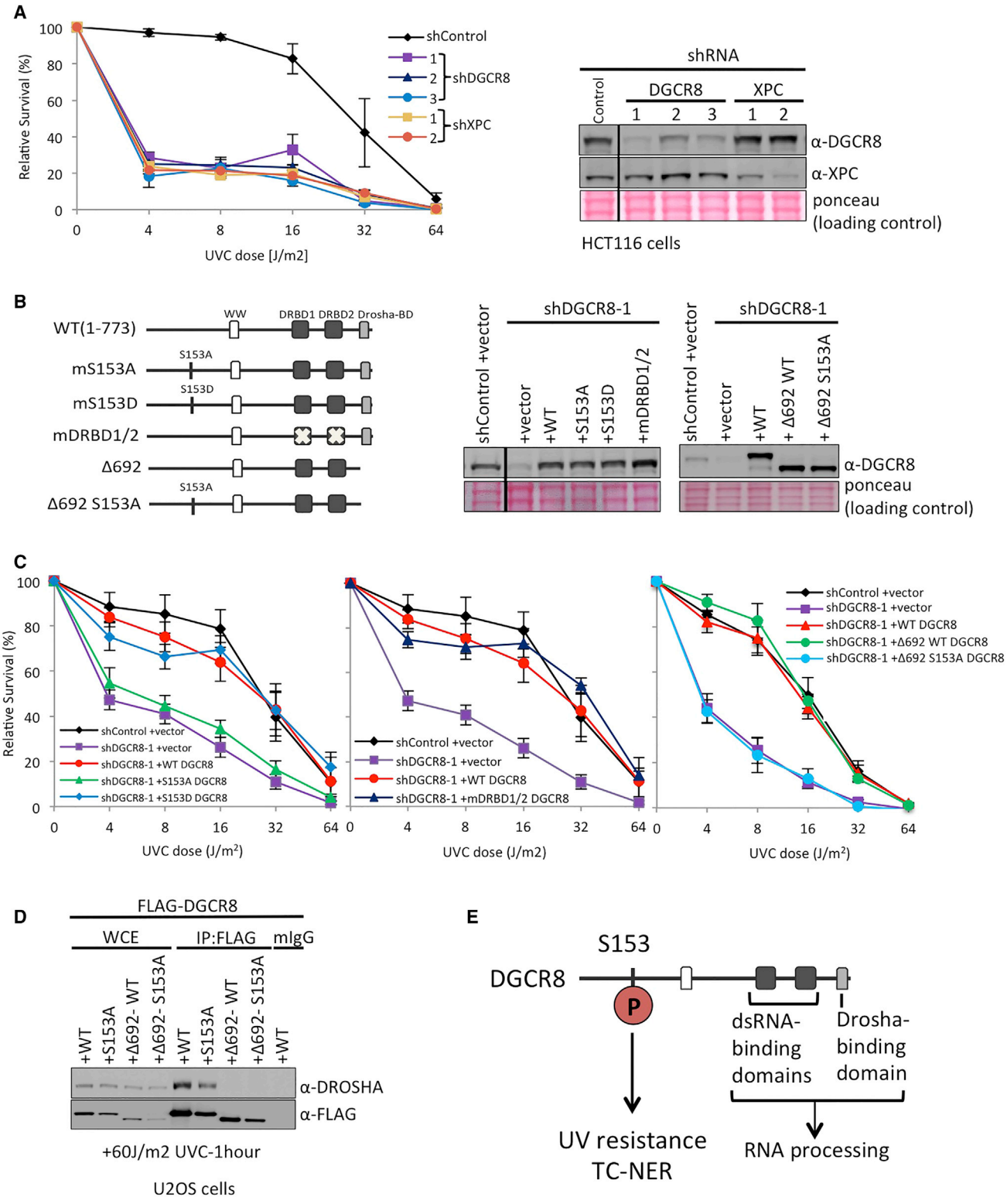

Figure 2. Phosphorylation of S153 on DGCR8 Is Critical for UV Resistance

(A) UV-C sensitivity assay. HCT116 cells were depleted of DGCR8 or XPC and plated for survival after UV irradiation or no radiation. The immunoblot shows DGCR8 and XPC depletion.

(B) Schematic of DGCR8 mutants. The immunoblot shows expression of the indicated shRNA-resistant DGCR8 constructs in DGCR8-depleted HCT116 cells.

(legend continued on next page)

372 human miRNAs in DGCR8-depleted HCT116 cells transduced with either empty vector, wild-type DGCR8, or the S153A mutant. DGCR8-depleted cells transduced with empty vector showed reduction of miRNA expression compared with non-depleted control or wild-type DGCR8-expressing cells, but there was no clear difference in the miRNA expression profiles between wild-type DGCR8 and S153A DGCR8 cells (Figure S3), suggesting that S153 is not critical for miRNA processing. This is consistent with a recent report that many phosphorylation sites on DGCR8 (including S153) are not critical for its miRNA processing activity (Herbert et al., 2013). These results indicate that the human DGCR8 protein has at least two independent functions: S153 phosphorylation-mediated UV resistance and RNA binding and Drosha binding domain-mediated RNA processing (Figure 2E).

DGCR8 Phosphorylation Mediates the Repair of UV-Induced DNA Lesions

We next measured the removal of CPDs and 6-4PPs after UV irradiation to test whether DGCR8 and Drosha are involved in the repair of UV-induced DNA lesions. DGCR8 depletion as well as XPC depletion and CSB depletion, reduced the removal of CPDs and 6-4PPs (Figure 4A; Figures S4A and S4B). Reintroduction of wild-type DGCR8 into DGCR8-depleted cells restored the efficient removal of CPDs and 6-4 PPs, whereas the S153A-DGCR8 mutant failed to do so, suggesting that UV-induced S153 phosphorylation is required for the efficient repair of UV-induced DNA lesions. In contrast, depletion of Drosha did not reduce the removal (Figure 4A; Figures S4A and S4B), suggesting that Drosha is not involved in the repair of the UV-induced DNA lesions. The mechanisms by which DGCR8 and Drosha function in UV resistance are therefore distinct.

DGCR8 and Factors Involved in TC-NER Are Epistatic in UV Sensitivity

To test whether DGCR8 is involved in NER and to identify in which NER subpathway it may be involved, we performed epistasis analyses (Figure 4B; Figure S4C). We depleted DGCR8 in human patient-derived fibroblasts deficient in XPC, XPA, CSA, or CSB and their corrected counterparts. As expected, XPC-, XPA-, CSA-, and CSB-deficient cells were hypersensitive to UV-C (Yasuda et al., 2007) and DGCR8 depletion-sensitized control (corrected) fibroblasts to UV-C. DGCR8 depletion further sensitized XPC-deficient cells to UV-C, indicating that DGCR8 is not epistatic with XPC, a factor specifically involved in GG-NER. In contrast, DGCR8 depletion did not further sensitize CSB-, CSA-, or XPA-deficient fibroblasts to UV-C, indicating that DGCR8 is epistatic with CSB, CSA, and XPA. CSB and CSA are factors specifically involved in TC-NER, whereas XPA is involved in both TC-NER and GG-NER. Therefore, these data collectively suggest that DGCR8 functions in TC-NER but not in GG-NER.

DGCR8 Phosphorylation Modulates RRS after UV Radiation

To confirm the involvement of DGCR8 in TC-NER, we utilized a recovery of RNA synthesis (RRS) assay (Jia et al., 2015; Figure 4C; Figure S4D). DGCR8-depleted cells showed impaired RRS after UV radiation, similarly to CSB-depleted cells. Reintroduction of either the wild-type or S153D DGCR8, but not S153A DGCR8, into DGCR8-depleted cells rescued RRS after UV radiation, suggesting that S153 phosphorylation is critical for RRS after UV radiation. These findings are consistent with DGCR8 being involved in TC-NER.

Because RNAPII stalling is presumed to be the initial step for TC-NER (Fousteri et al., 2006), we hypothesized that RNAPII stalling triggers S153 phosphorylation. To test this, we treated human cells with a transcription elongation inhibitor, 5,6-dichlorobenzimidazole 1-β-D-ribofuranoside (DRB). DRB treatment led to increased S153 phosphorylation even in the absence of UV treatment (Figure 4D). Depletion of CDK9, a kinase involved in transcription elongation and a target of DRB, also led to increased phosphorylation of S153 (Figure 4D). These findings suggest that RNAPII stalling caused either by UV-induced DNA lesions or by other mechanisms stimulates S153 phosphorylation.

Furthermore, wild-type DGCR8 was co-immunoprecipitated with RNAPII, CSB, and Drosha (Figures 5A and 5B), but not with XPC (Figure S4E), regardless of UV treatment, consistent with DGCR8's role in TC-NER. Interestingly, S153A-DGCR8 was also co-immunoprecipitated with RNAPII, CSB, and Drosha (Figures 5A and 5B), indicating that S153 phosphorylation is not critical for the interactions among these factors. CSA or CSB deficiency did not affect UV-induced phosphorylation of S153 (Figure S5A), indicating that S153 phosphorylation is not downstream of CSA or CSB. Furthermore, DGCR8 depletion did not affect the expression of CSA, CSB, or RNAPII (Figure S5B). Therefore, although DGCR8 is involved in TC-NER, its precise mechanism remains to be determined.

Lastly, we sought to identify the kinase that phosphorylates S153 of DGCR8 in response to UV treatment. Because c-*jun* N-terminal kinases (JNKs) are known to be activated in response to UV exposure (Johnson and Nakamura, 2007; López-Camarillo et al., 2012), we focused on JNKs. First, treatment with a JNK inhibitor, SP600125, abrogated UV-induced S153 phosphorylation (Figure 6A), whereas treatment with a JNK activator, anisomycin, induced S153 phosphorylation in the absence of UV treatment (Figure 6B). Second, overexpression of JNK1a1 induced S153 phosphorylation even in untreated cells, and the phosphorylation was sustained after UV radiation (Figure 6C).

(C) UV-C sensitivity assay. DGCR8-depleted HCT116 cells were transduced with the indicated DGCR8 constructs and plated for survival after UV irradiation or no radiation. All UV-C sensitivity data represent mean values ± SEM of three independent experiments.
(D) IP western blot. Cell lysates of UV-treated U2OS cells transduced with the indicated FLAG-tagged DGCR8 constructs were immunoprecipitated with anti-FLAG. The immunoblot was done using the indicated antibodies.
(E) Model for two independent functions of DGCR8: S153 phosphorylation-mediated UV resistance and TC-NER and dsRNA binding domain- and Drosha binding domain-mediated RNA processing.
See also Figures S2 and S3.

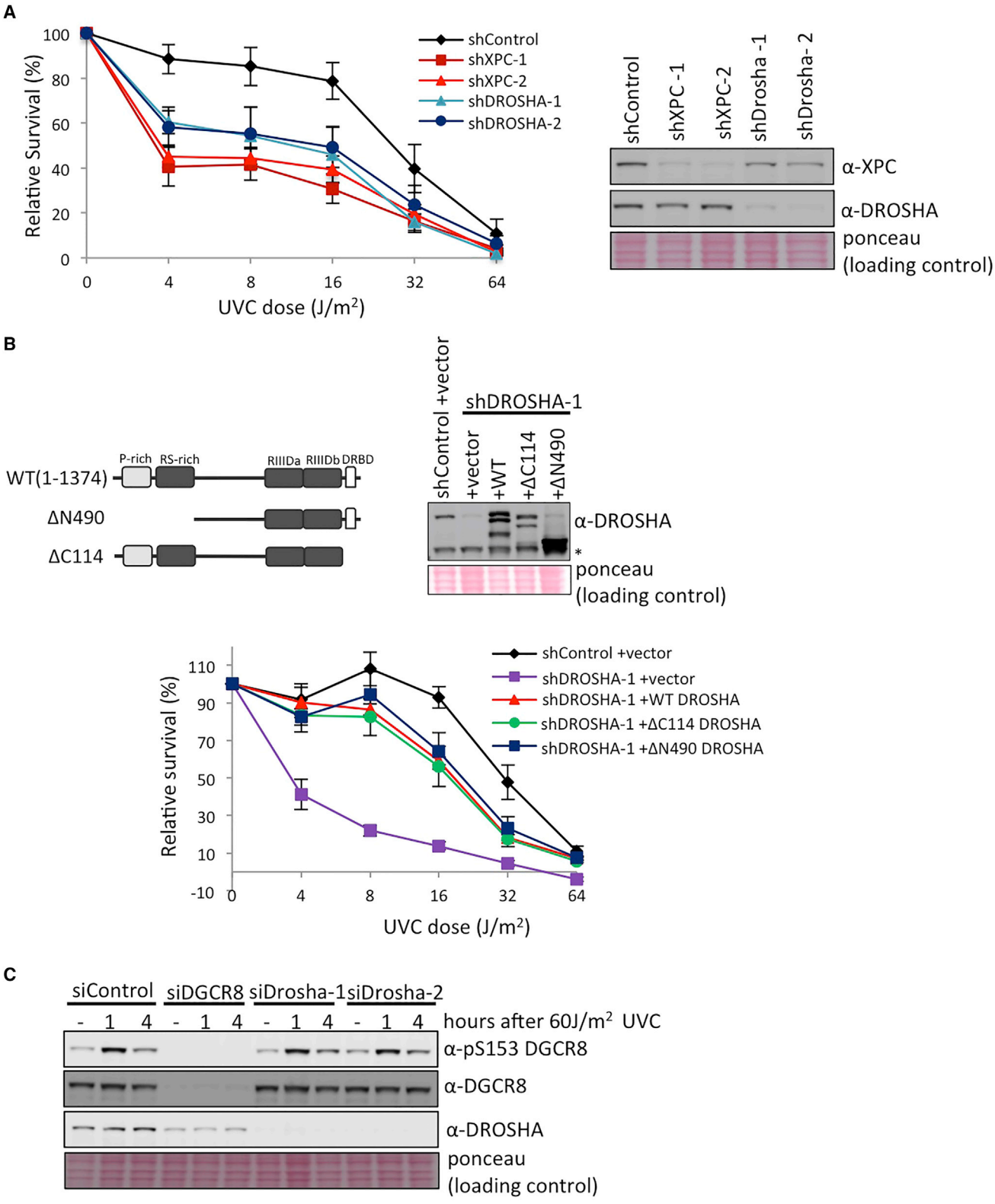

Figure 3. Drosha Is Required for UV Resistance Independently of DGCR8

(A) UV-C sensitivity assay. HCT116 cells were depleted of Drosha or XPC and plated for survival after ± UV irradiation. The immunoblot shows Drosha and XPC depletion.

(legend continued on next page)

To determine whether JNK directly phosphorylates S153 of DGCR8, we conducted an in vitro kinase assay using glutathione S-transferase (GST)-tagged wild-type or S153A fragments (amino acids [aa] 1–275) of DGCR8 or GST-tagged (aa 1–79) C-JUN (positive control) as substrates and immunopurified FLAG-WT-JNK1a1 or kinase-dead FLAG-JNK1a1 (APF) from cells treated with and without UV radiation (Figure S6A). As expected, wild-type (WT)-JNK1a1, but not kinase-dead JNK1a1, phosphorylated S63 of C-JUN (Figure S6B). Importantly, WT-JNK1a1 from UV-treated cells phosphorylated S153 of WT-DGCR8 in vitro (Figures 6D, lane 6, and 6E, lane 4), whereas the kinase-dead JNK1a1 was unable to phosphorylate S153 (Figure 6E, lanes 5 and 6). Taken together, these data suggest that JNKs phosphorylate S153 of DGCR8 in response to UV radiation.

DISCUSSION

Based on these findings, we propose a cellular signaling pathway (the DGCR8-mediated UV response pathway) that connects UV-induced DNA damage, DGCR8 protein, and TC-NER (Figure 6F). In this pathway, in response to UV radiation, RNAPII stalls and triggers phosphorylation of S153 of DGCR8 by JNKs, and this phosphorylation facilitates the efficient removal of UV-induced DNA lesions through TC-NER in a manner independent of miRNA processing and Drosha. This function is, in turn, important for cellular survival after UV exposure. Drosha also contributes to cellular resistance to UV, but by mechanisms that are independent of DNA repair.

The JNKs are stress-activated kinases that are a part of the MAPK family. JNKs are stimulated by a plethora of intrinsic and extrinsic stimuli, including UV exposure (Johnson and Nakamura, 2007; López-Camarillo et al., 2012). DGCR8 has been shown to be multiply phosphorylated by ERK/MAPK, which affects pro-growth miRNA processing (Herbert et al., 2013). Our studies suggest that a single UV-induced phosphorylation site, S153, is critical for UV resistance and that JNKs phosphorylate S153 of DGCR8 in response to UV exposure. These findings suggest that DGCR8 is one of the critical substrates of JNKs in the cellular response to UV exposure. Because S153 phosphorylation was not completely inhibited in the presence of a JNK inhibitor (Figure 6A), it is likely that some other kinases also phosphorylate S153 of DGCR8. It has been reported that simple inhibition of JNKs does not affect the removal of UV-induced DNA lesions (Rouget et al., 2008), which also suggests the involvement of some additional kinases in the phosphorylation of S153. Such kinases remain to be determined. Treatment with cisplatin or mitomycin C did not induce S153 phosphorylation (Figure S1E), whereas it has been reported that such a treatment activates JNKs, suggesting that activation of JNKs is not sufficient to induce S153 phosphorylation and that there should be more complex regulatory mechanisms of this process.

We found that DGCR8 is involved in TC-NER and that DGCR8 physically interacts with some known factors involved in TC-NER. However, the precise molecular mechanism by which S153 phosphorylation on DGCR8 regulates TC-NER remains to be determined. Elucidating this mechanism is a focus of our on-going research. S153-phosphorylated DGCR8 may facilitate the recruitment of known or unknown factors involved in TC-NER to stalled RNAPII and mediate the removal of UV-induced DNA lesions. S153-phosphorylated DGCR8 may regulate interaction among TC-NER factors or some post-translational modifications of TC-NER factors. Another possibility is that S153-phosphorylated DGCR8 may sequester some negative regulators of TC-NER. The microprocessor complex is recruited to chromatin during transcription and processes pri-miRNA co-transcriptionally (Morlando et al., 2008; Pawlicki and Steitz, 2008). It would be of interest to test whether S153-phosphorylated DGCR8 affects the recruitment of any TC-NER factors to RNAPII. However, our functional and epistasis studies, in addition to the physical interactions that we have identified between DGCR8 and TC-NER factors, support a completely biological function of DGCR8 in the UV damage response that is independent of miRNA processing. On the other hand, it is still possible that some miRNAs regulate TC-NER because generation of some miRNAs is not DGCR8-dependent (Chong et al., 2010; Berezikov et al., 2007).

Our studies, along with other studies, suggest that factors involved in miRNA processing function in DNA repair and DNA damage response. Deletion of Dicer or Dgcr8 in the developing mouse brain leads to increased DNA damage (Swahari et al., 2016). Furthermore, small non-coding RNAs, termed DNA damage response RNAs (DDRNAs) or double-strand break (DSB)-induced RNAs (diRNAs), generated at sites of DNA damage, are involved in DNA damage response after DSB generation (Francia et al., 2012, 2016; Wei et al., 2012). These small non-coding RNAs are generated in a manner dependent on Drosha and Dicer. How these small non-coding RNAs interact with the DGCR8-mediated UV response pathway is an interesting issue. Current evidence suggests that they are differently regulated: generation of DDRNAs presumably depends on the RNA processing activity of Drosha and Dicer, whereas the DGCR8-mediated UV response pathway and cellular resistance to UV did not require the RNA processing activity of the DGCR8-Drosha complex (Figure 2C; Figure S3). Therefore, we assume that they have distinct functions: DDRNAs are important for DNA damage response after DSB but may not be important for UV resistance or TC-NER, whereas the DGCR8-mediated UV response pathway is critical for TC-NER.

The mechanism by which Drosha supports UV resistance is unknown. This is a non-canonical function of Drosha because it did not require DGCR8 binding or miRNA processing activities.

(B) Schematic of Drosha mutants. The immunoblot confirmed expression of the indicated Drosha constructs in Drosha-depleted HCT116 cells. Drosha-depleted HCT116 cells were transduced with the indicated Drosha constructs and subjected to the UV-C sensitivity assay. All UV-C sensitivity data represent mean values ± SEM of three independent experiments.
(C) U2OS cells depleted of DGCR8 or Drosha were UV-irradiated and subjected to immunoblotting with the indicated antibodies.
See also Figure S2.

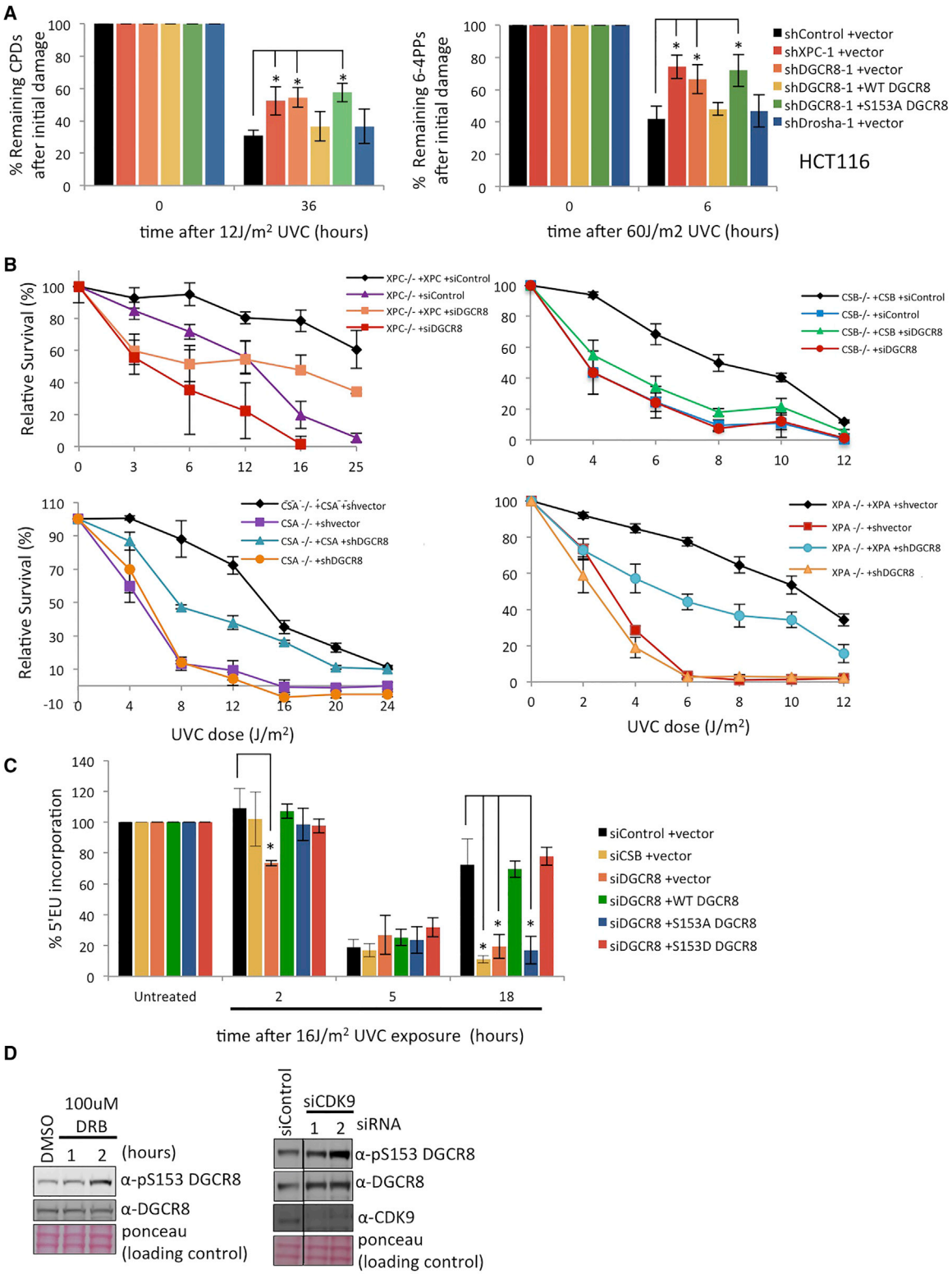

Figure 4. Phosphorylation of S153 on DGCR8 Is Involved in TC-NER

(A) Removal of CPDs or 6-4PPs assessed by flow cytometry using anti-CPD and anti-6-4PP antibodies. HCT116 cells depleted of the indicated genes and complemented with the indicated constructs were treated with UV-C, and CPD-positive cells and 6-4PP-positive cells at the indicated time points were measured. Asterisks indicate a significant difference ($p < 0.05$) relative to shControl and empty vector-transduced cells.

(legend continued on next page)

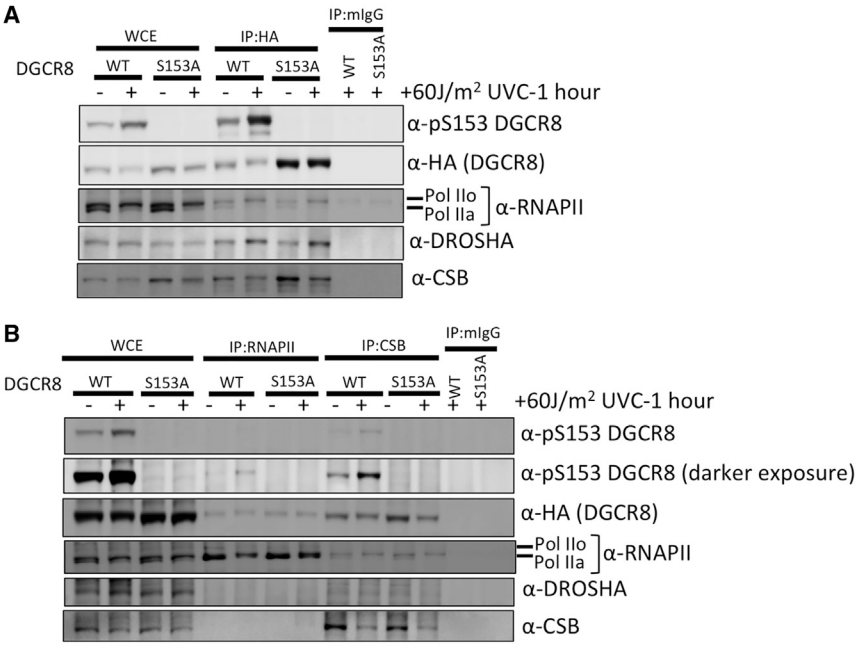

Figure 5. DGCR8 Interacts with Factors Involved in TC-NER

(A and B) IP western blots. Cell lysate of UV-treated (or untreated) U2OS cells transduced with the HA-tagged DGCR8 (wild-type or S153A mutant) constructs were immunoprecipitated with the indicated antibodies. The immunoblot was done using the indicated antibodies. (A) IP was done using anti-HA antibody. (B) IP was done using anti-RNAPII and anti-CSB antibodies.

See also Figures S4 and S5.

It may be related to UV tolerance mechanisms other than DNA repair itself, such as translesion synthesis and suppression of apoptosis.

Our discovery of a miRNA processing-independent function of DGCR8 has several important implications. In humans, DGCR8 is one of the many genes whose heterozygous deletion is associated with DiGeorge syndrome, characterized by developmental abnormalities and behavioral problems (Shiohama et al., 2003). S153-mediated function may or may not contribute to the clinical phenotypes of DiGeorge syndrome and schizophrenia (Zhou et al., 2013), for which SNPs in the microprocessor complex are associated with increased risk. The fact that DiGeorge syndrome is not associated with UV sensitivity suggests that Dgcr8 heterozygosity does not cause a sufficient loss of function to confer this phenotype. Whether mutations in any genes involved in the DGCR8-mediated UV response pathway cause XP, CS, COFS, UVSS, and TTD is another important question. Somatic mutations in the catalytic domains of Drosha and DGCR8 occur in Wilms tumors (Torrezan et al., 2014). These mutations affect the miRNA processing activity of the microprocessor complex and are unlikely to affect S153 phosphorylation. However, the cBioPortal for Cancer Genomics (http://www.cbioportal.org/; Cerami et al., 2012) revealed several mutations throughout the DGCR8 gene in human cancers. Some of the missense mutations, for example, L152F, S156N (melanoma), and G149C (stomach and lung cancer), flank S153. It remains to be tested whether these mutations alter S153-mediated function.

Multiple Dgcr8-deficient mouse models have been developed (Bezman et al., 2010; Rao et al., 2009; Wang et al., 2007; Yi et al., 2009) with the assumption that DGCR8 functions only in RNA processing. Our results suggest that it is important to determine whether the phenotypes observed in these animal models are mediated by the RNA processing function or the S153-mediated TC-NER function of Dgcr8.

Thus, further elucidation of the non-canonical functions of the microprocessor complex proteins is warranted for our understanding of many diseases.

EXPERIMENTAL PROCEDURES

Cell Lines

U2OS, HeLa, and HCT116 cells were obtained from the ATCC. MEFs were a gift from Bruce Clurman's lab (Fred Hutchinson Cancer Research Center [FHCRC]). Immortal human keratinocytes (HaCaT) were a gift from Paul Nghiem's lab (University of Washington). Primary human foreskin fibroblasts (HFFs) were a gift from Denise Galloway's lab (FHCRC). XPA-deficient (GM04312), XPA-corrected (GM15876), CSA-deficient (GM16094), and CSB-deficient (GM16095) human fibroblasts were purchased from Coriell Cell Repositories. XPC-deficient cells (XP4PASV) and XPC-corrected human fibroblasts (XP4PASV/FLAG-XPC(WT)) were described previously (Yasuda et al., 2007). Dgcr8 knockout MEFs were purchased from Novus Biologicals and cultured according to the manufacturer's specifications. All cells were maintained at 37°C in a 5% CO_2 incubator and grown in DMEM containing 10% fetal bovine serum (FBS), L-glutamine, and penicillin/streptomycin (Pen/Strep). 10 μg/mL of hygromycin B (Life Technologies) was added to the medium for XPC cells.

Plasmids, Small Interfering RNAs, shRNAs, and Virus Production

FLAG- or hemagglutinin (HA)-tagged human and mouse DGCR8 and FLAG-tagged-human CSA cDNA were cloned into the Nco1 and BamH1 sites of

(B) UV-C sensitivity assay. XPC-, CSA-, CSB-, or XPA-deficient fibroblasts and their corrected counterparts were depleted of DGCR8 and plated for survival after UV-C irradiation or no radiation.

(C) RRS assay. 5′EU incorporation kinetics after UV-C irradiation. U2OS cells transfected with the indicated siRNAs and cDNA constructs were subjected to the assay. Asterisks indicate a significant difference ($p < 0.05$) relative to siControl and empty vector-transduced cells.

(D) U2OS cells treated with DRB or transfected with CDK9 siRNA were immunoblotted with the indicated antibodies.

All data represent mean values ± SEM of three independent experiments.

See also Figure S4.

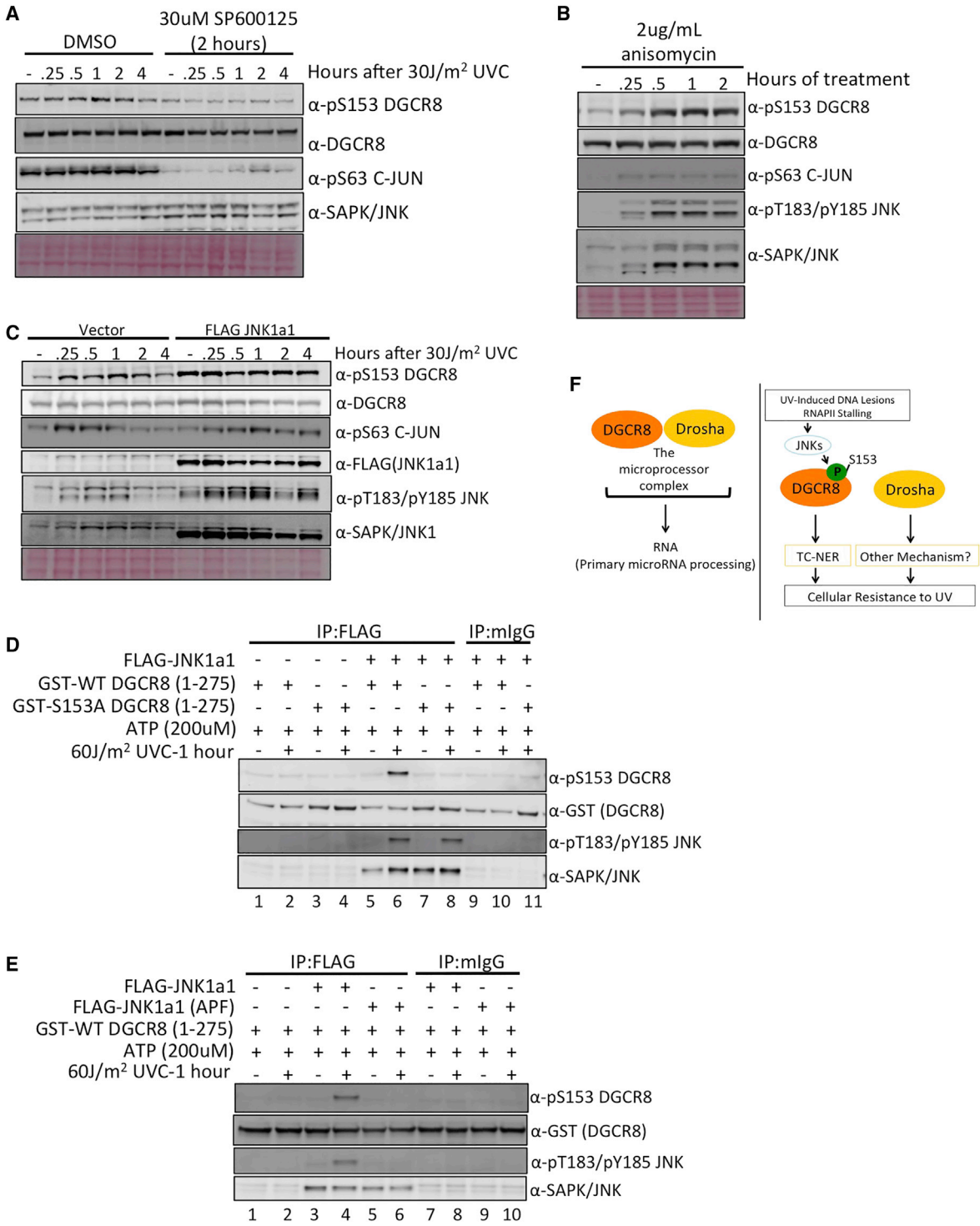

Figure 6. JNK Phosphorylates S153 of DGCR8 after UV Radiation

(A) Immunoblot. U2OS cells were pretreated with the JNK inhibitor SP600125 or DMSO for 2 hr, irradiated with UV or not, and incubated with medium containing SP600125 or DMSO, and then cell lysates were harvested at the indicated time points.

(B) Immunoblot. U2OS cells were continuously treated with the JNK activator anisomycin, and cell lysates were harvested at the indicated time points.

(C) Immunoblot. U2OS cells expressing either vector or FLAG-JNK1a1 were treated with UV or left untreated, and cell lysates were harvested at the indicated time points.

(legend continued on next page)

the pMMP-IRES-puro retroviral vector (Pulsipher et al., 1998). Phosphomutants (S95A, S153A, S271A, S275A, T371A, S373A, S377A, S434A, and S619A) and a phosphomimic mutant (S153D) of DGCR8 were generated using the QuikChange XL site-directed mutagenesis kit (200514-5, Agilent Technologies). The double-stranded RNA binding domain mutant A568K, A569K, A676K, S677K (mDRBD1/2) of DGCR8 was subcloned into pMMP-IRES-puro using the aforementioned sites from pcDNA-mDRBD1/2 DGCR8 (Yeom et al., 2006), a gift from the Narry Kim lab (Seoul National University). FLAG-DGCR8 WT and mutants were mutated using the QuikChange XL site-directed mutagenesis kit with primers (forward, 5′CTCCCTGCTGAG GACCCTTTTAATTTTTATGGGGCCTCCCTTCTC

TCCAAAGGA-3′; reverse, 5′TCCTTTGGAGAGAAGGGAGGCCCCATAAAA ATTAAAAGGGTCCTCAGCAGGGAG-3′) to generate shDGCR8-1-resistant constructs. The Drosha-binding domain mutants (FLAG-Δ692 WT and FLAG-Δ692 S153A) of DGCR8 were also subcloned into pMMP-IRES-puro. FLAG-wild-type-, FLAG-ΔC114-, and FLAG-ΔN490-Drosha were subcloned into the pBABE puro retroviral vector (a gift from Bruce Clurman's lab, FHCRC) using BamH1 and Sal1 sites from plasmids (Lee et al., 2006) provided by the Narry Kim lab. The CSB construct (pBR-CSB) was a gift from Alan Weiner's lab (University of Washington) and was used to subclone FLAG-CSB into the pBabe-puro retroviral vector using BamH1 and Sal1 sites. pCDNA3 FLAG Jnk1a1 (Addgene plasmid # 13798) and pCDNA3 FLAG Jnk1a1(apf) (Addgene plasmid # 13846) were a gift from the Roger Davis lab (University of Massachusetts). Retroviruses and lentiviruses were produced as described previously (Wang et al., 2011). All constructs were verified by direct sequencing.

Mass Spectrometry

HeLa cells stably infected with pMMPpuroFLAG-DGCR8 were treated with 60 J/m^2 of UV-C, and 1 hr later, whole-cell extracts were prepared in lysis buffer. Immunoprecipitation (IP) was performed using a monoclonal antibody against FLAG (M2, Santa Cruz Biotechnology), and the IP product was separated by 7.5% SDS-PAGE. Gel pieces corresponding to FLAG-DGCR8 bands were cut from a Coomassie-stained gel and subjected to tryptic digestion (Shevchenko et al., 1996). Tryptic peptides were concentrated and desalted using a C18micro ZipTip (Millipore) following the manufacturer's instructions. The eluted peptides were dried by vacuum centrifugation, resuspended in 7 μL of 2% acetonitrile/0.1% formic acid, and 5 μL was analyzed by liquid chromatography-tandem mass spectrometry (LC-MS/MS) with a nanoLC 2D (Eksigent Technologies) coupled to an OrbiTrap mass spectrometer (Thermo Scientific) using an instrument configuration (Licklider et al., 2002).

Western Blot Analysis

Whole-cell lysates were prepared using sample buffer (0.05 mol/L Tris-HCl [pH 6.8], 2% SDS, and 6% β-mercaptoethanol), resolved by polyacrylamide gel (NuPage, Life Technologies) electrophoresis, and transferred onto nitrocellulose membranes. Chemiluminescence was used for detection, and membranes were digitally scanned by Imagequant LAS 4000 (GE Biosciences).

Immunofluorescent Microscopy

To detect pS153 DGCR8 by immunofluorescence, cells were treated with 60 J/m^2 UV-C. After 1 hr, cells were fixed with 4% paraformaldehyde (Santa Cruz Biotechnology) for 10 min at room temperature and subsequently permeabilized with PBS containing 0.5% Tween 20 (Fisher Scientific) for 10 min at room temperature. After several washes with PBS containing 0.5% Tween 20 (washing buffer), cells were incubated overnight at 4°C with anti-phosphoS153 (1:1,000). After several washes with PBS containing 0.5% Tween 20, cells were incubated with Alexa Fluor 488 goat anti-rabbit (A11034, Life Technologies) secondary antibody for 1 hr. Nuclei were counterstained with DAPI (1 μg/mL). Coverslips were mounted on slides in Vectashield (Vector Laboratories). Image acquisitions were made with a TE2000 Nikon microscope equipped with a 20× immersion objective and a charge-coupled device (CCD) camera (CoolSNAP ES, Photometrics).

Flow Cytometry

Cells were treated with UV-C (12 J/m^2 for detection of CPDs or 60 J/m^2 for detection of 6-4PPs) and fixed with 2% paraformaldehyde at 37°C for 10 min. Then cells were treated with cold 90% methanol for 30 min at −20°C and treated with DNase (Promega) for 1 hr at 37°C. After blocking with PBS containing 1% BSA for 10 min at room temperature, cells were incubated with anti-CPD (1:1,000) or anti-6-4PPs (1:1,000) diluted in PBS containing 1% BSA and 0.25% Tween 20 overnight at 4°C. After washing with PBS containing 1% BSA and 0.05% Tween 20, cells were incubated with fluorescein-conjugated anti-mouse antibody (1:1,000) (715-095-151, Jackson ImmunoResearch) for 1 hr in the dark at room temperature. Nuclei were counterstained with propidium iodide (2 μg/mL, P1470, Sigma-Aldrich) and treated with RNase A (100 μg/mL, Invitrogen) for 20 min at 37°C. Flow cytometric analyses were conducted with a BD FACS Canto II analyzer and FlowJo software.

RRS Assay

RRS assays were done as described with some modifications (Jia et al., 2015; Nakazawa et al., 2010). U2OS cells stably expressing small interfering RNA (siRNA)-resistant FLAG-WT DGCR8, FLAG-S153A DGCR8, or FLAG-S153D-DGCR8 were transfected with siRNA against endogenous DGCR8. Forty-eight hours after transfection of siRNAs, cells were irradiated with UV-C (16 J/m^2) and immediately incubated with 5′-ethynyuridine (5′EU) (50 μM, Life Technologies) for 2 hr (Jia et al., 2015; Nakazawa et al., 2010). Then cells were fixed and permeabilized at the indicated time points. After blocking with PBS containing 10% FBS, cells were incubated for 1 hr at room temperature with Alexa Fluor 488 goat anti-rabbit (A11034, Life Technologies) secondary antibody. Nuclei were counterstained with DAPI (1 μg/mL).

Purification of Recombinant GST-DGCR8 Protein and In Vitro Kinase Assay

The DNA fragment corresponding to aa 1–275 FLAG-tagged WT or S153A DGCR8 was cloned into the pGEX-4T-1 vector (GE Healthcare). The recombinant plasmids were transformed into *E. coli* BL21 (DE3) cells (EMD Millipore). GST-DGCR8-WT and GST-DGCR8-S153A proteins were expressed and purified using GST-Bind resin (EMD Millipore) according to the manufacturer's instructions. Human JUN partial-length recombinant protein (aa 1–79) with a GST tag (Novus Biologicals) was used a positive control. The in vitro kinase assay was performed as described previously (Chadee and Kyriakis, 2010).

Cell Survival Assay

Cells were seeded into 12-well plates at 8 × 10^3/well (HCT-116), 1 × 10^4/well (U2OS), and 1 × 10^4/well (XP and CS fibroblasts) and treated with UV-C (254 nm) from a UV Stratalinker 1800 (Stratagene) or UV-B (output range, 280–320 nm) at the indicated doses using a method described previously (Wallace et al., 2012). After incubation for 5–7 days, cells were stained with crystal violet as described previously (Wang et al., 2011).

Statistics

All statistical analyses were done using Student's t test (two-tailed). $p < 0.05$ was considered significant.

(D) Immunoblot after the in vitro kinase assay. A recombinant GST-tagged WT or S153A DGCR8 (aa 1–275) fragment was used as a substrate, and immunopurified WT JNK1a1 was used as the enzyme.
(E) Immunoblot after the in vitro kinase assay. Recombinant GST-tagged WT DGCR8 (aa 1–275) fragment was used as a substrate, and immunopurified WT JNK1a1 or kinase-dead JNK1a1 (APF) was used as the enzyme.
(F) Schematic of DGCR8 and Drosha functions. The DGCR8-Drosha microprocessor complex processes RNAs. When DNA is damaged by UV radiation, RNAPII stalls and triggers phosphorylation of S153 on DGCR8, which facilitates removal of UV-induced DNA lesions by TC-NER and promotes UV resistance. Drosha is also involved in UV resistance by an unknown mechanism.
See also Figure S6.

miRNA Profiling

RNA from stable isogenic cell lines (HCT-116) depleted of endogenous DGCR8 by shDGCR8-1, transduced with shRNA-resistant FLAG-WT, FLAG-S153A DGCR8, or empty vector, were extracted using the RNeasy mini kit (QIAGEN). RNA from four biological replicates were submitted to Exiqon for miRNA real-time PCR using miRCURY LNA Universal RT miRNA PCR Human Panel 1, which contains 372 human miRNAs.

SUPPLEMENTAL INFORMATION

Supplemental Information includes Supplemental Experimental Procedures and six figures and can be found with this article online at http://dx.doi.org/10.1016/j.celrep.2017.03.021.

AUTHOR CONTRIBUTIONS

P.C.C. designed and performed experiments, analyzed data, and wrote the manuscript. K.K.D. analyzed data and wrote the manuscript. N.T. performed experiments and analyzed data. Y.C. and B.E.C. provided technical advice and generated reagents. M.K. and P.N. provided technical advice and input for interpretation and edited the manuscript. J.H., Y.W., and C.J. provided technical advice and input for interpretation. P.R.G. performed mass spectrometry, analyzed data, and wrote the manuscript. K.S. and M.S. provided technical advice and input for interpretation. T.T. conceptualized and directed the study, analyzed data, and wrote the manuscript.

ACKNOWLEDGMENTS

We thank Drs. Javier F Cáceres, Alan Weiner, Ronald Cheung, and Muneesh Tewari for critical reading of the manuscript and Kanan Lathia for technical assistance. We thank Drs. V. Narry Kim and Alan Weiner, the Galloway lab (FHCRC), and the Clurman lab (FHCRC) for reagents. This work was supported by Howard Hughes Medical Institute, the NIH/NHLBI (R21 HL092978 to T.T.), NIH/NCI (R01 CA125636 to T.T.), NIH/NIEHS (R21 ES026326 to T.T.), NIH/NIAMS (R01-AR049832 and R01-AR067722 to P.N.), the Fanconi Anemia Research Fund (to T.T.), and an Obliteride Pilot Grant (to T.T.). Y.W. was a research fellow supported by the Canadian Institute of Health Research. J.W. and P.C. were supported by PHS NRSA 2T32 GM007270 from NIGMS. K.D. is a Thomsen Breast Cancer Fellow. This work was supported by grants-in-aid to K.S. (JSPS KAKENHI Grants JP16H06307 and JP16H01311). The Fred Hutch Proteomics Facility is partially funded by Cancer Center Support Grant P30 CA015704 from the NIH.

Received: September 25, 2016
Revised: December 24, 2016
Accepted: March 3, 2017
Published: April 4, 2017

REFERENCES

Berezikov, E., Chung, W.J., Willis, J., Cuppen, E., and Lai, E.C. (2007). Mammalian mirtron genes. Mol. Cell *28*, 328–336.

Bezman, N.A., Cedars, E., Steiner, D.F., Blelloch, R., Hesslein, D.G., and Lanier, L.L. (2010). Distinct requirements of microRNAs in NK cell activation, survival, and function. J. Immunol. *185*, 3835–3846.

Carthew, R.W., and Sontheimer, E.J. (2009). Origins and Mechanisms of miRNAs and siRNAs. Cell *136*, 642–655.

Cerami, E., Gao, J., Dogrusoz, U., Gross, B.E., Sumer, S.O., Aksoy, B.A., Jacobsen, A., Byrne, C.J., Heuer, M.L., Larsson, E., et al. (2012). The cBio cancer genomics portal: an open platform for exploring multidimensional cancer genomics data. Cancer Discov. *2*, 401–404.

Chadee, D.N., and Kyriakis, J.M. (2010). Activation of SAPK/JNKs in vitro. Methods Mol. Biol. *661*, 59–73.

Cheng, T.L., Wang, Z., Liao, Q., Zhu, Y., Zhou, W.H., Xu, W., and Qiu, Z. (2014). MeCP2 suppresses nuclear microRNA processing and dendritic growth by regulating the DGCR8/Drosha complex. Dev. Cell *28*, 547–560.

Chong, M.M., Zhang, G., Cheloufi, S., Neubert, T.A., Hannon, G.J., and Littman, D.R. (2010). Canonical and alternate functions of the microRNA biogenesis machinery. Genes Dev. *24*, 1951–1960.

Dziunycz, P., Iotzova-Weiss, G., Eloranta, J.J., Läuchli, S., Hafner, J., French, L.E., and Hofbauer, G.F. (2010). Squamous cell carcinoma of the skin shows a distinct microRNA profile modulated by UV radiation. J. Invest. Dermatol. *130*, 2686–2689.

Fousteri, M., Vermeulen, W., van Zeeland, A.A., and Mullenders, L.H. (2006). Cockayne syndrome A and B proteins differentially regulate recruitment of chromatin remodeling and repair factors to stalled RNA polymerase II in vivo. Mol. Cell *23*, 471–482.

Francia, S., Michelini, F., Saxena, A., Tang, D., de Hoon, M., Anelli, V., Mione, M., Carninci, P., and d'Adda di Fagagna, F. (2012). Site-specific DICER and DROSHA RNA products control the DNA-damage response. Nature *488*, 231–235.

Francia, S., Cabrini, M., Matti, V., Oldani, A., and d'Adda di Fagagna, F. (2016). DICER, DROSHA and DNA damage response RNAs are necessary for the secondary recruitment of DNA damage response factors. J. Cell Sci. *129*, 1468–1476.

Han, J., Lee, Y., Yeom, K.H., Kim, Y.K., Jin, H., and Kim, V.N. (2004). The Drosha-DGCR8 complex in primary microRNA processing. Genes Dev. *18*, 3016–3027.

Hanawalt, P.C., and Spivak, G. (2008). Transcription-coupled DNA repair: two decades of progress and surprises. Nat. Rev. Mol. Cell Biol. *9*, 958–970.

Herbert, K.M., Pimienta, G., DeGregorio, S.J., Alexandrov, A., and Steitz, J.A. (2013). Phosphorylation of DGCR8 increases its intracellular stability and induces a progrowth miRNA profile. Cell Rep. *5*, 1070–1081.

Herrlich, P., Karin, M., and Weiss, C. (2008). Supreme EnLIGHTenment: damage recognition and signaling in the mammalian UV response. Mol. Cell *29*, 279–290.

Iorio, M.V., and Croce, C.M. (2012). MicroRNA dysregulation in cancer: diagnostics, monitoring and therapeutics. A comprehensive review. EMBO Mol. Med. *4*, 143–159.

Jia, N., Nakazawa, Y., Guo, C., Shimada, M., Sethi, M., Takahashi, Y., Ueda, H., Nagayama, Y., and Ogi, T. (2015). A rapid, comprehensive system for assaying DNA repair activity and cytotoxic effects of DNA-damaging reagents. Nat. Protoc. *10*, 12–24.

Johnson, G.L., and Nakamura, K. (2007). The c-jun kinase/stress-activated pathway: regulation, function and role in human disease. Biochim. Biophys. Acta *1773*, 1341–1348.

Lee, Y., Han, J., Yeom, K.H., Jin, H., and Kim, V.N. (2006). Drosha in primary microRNA processing. Cold Spring Harb. Symp. Quant. Biol. *71*, 51–57.

Licklider, L.J., Thoreen, C.C., Peng, J., and Gygi, S.P. (2002). Automation of nanoscale microcapillary liquid chromatography-tandem mass spectrometry with a vented column. Anal. Chem. *74*, 3076–3083.

López-Camarillo, C., Ocampo, E.A., Casamichana, M.L., Pérez-Plasencia, C., Alvarez-Sánchez, E., and Marchat, L.A. (2012). Protein kinases and transcription factors activation in response to UV-radiation of skin: implications for carcinogenesis. Int. J. Mol. Sci. *13*, 142–172.

Macias, S., Plass, M., Stajuda, A., Michlewski, G., Eyras, E., and Cáceres, J.F. (2012). DGCR8 HITS-CLIP reveals novel functions for the Microprocessor. Nat. Struct. Mol. Biol. *19*, 760–766.

Macias, S., Cordiner, R.A., and Cáceres, J.F. (2013). Cellular functions of the microprocessor. Biochem. Soc. Trans. *41*, 838–843.

Morlando, M., Ballarino, M., Gromak, N., Pagano, F., Bozzoni, I., and Proudfoot, N.J. (2008). Primary microRNA transcripts are processed co-transcriptionally. Nat. Struct. Mol. Biol. *15*, 902–909.

Nakazawa, Y., Yamashita, S., Lehmann, A.R., and Ogi, T. (2010). A semi-automated non-radioactive system for measuring recovery of RNA synthesis and

unscheduled DNA synthesis using ethynyluracil derivatives. DNA Repair (Amst.) *9*, 506–516.

Pawlicki, J.M., and Steitz, J.A. (2008). Primary microRNA transcript retention at sites of transcription leads to enhanced microRNA production. J. Cell Biol. *182*, 61–76.

Pothof, J., Verkaik, N.S., van IJcken, W., Wiemer, E.A., Ta, V.T., van der Horst, G.T., Jaspers, N.G., van Gent, D.C., Hoeijmakers, J.H., and Persengiev, S.P. (2009). MicroRNA-mediated gene silencing modulates the UV-induced DNA-damage response. EMBO J. *28*, 2090–2099.

Pulsipher, M., Kupfer, G.M., Naf, D., Suliman, A., Lee, J.S., Jakobs, P., Grompe, M., Joenje, H., Sieff, C., Guinan, E., et al. (1998). Subtyping analysis of Fanconi anemia by immunoblotting and retroviral gene transfer. Mol. Med. *4*, 468–479.

Rao, P.K., Toyama, Y., Chiang, H.R., Gupta, S., Bauer, M., Medvid, R., Reinhardt, F., Liao, R., Krieger, M., Jaenisch, R., et al. (2009). Loss of cardiac microRNA-mediated regulation leads to dilated cardiomyopathy and heart failure. Circ. Res. *105*, 585–594.

Rouget, R., Auclair, Y., Loignon, M., Affar, B., and Drobetsky, E.A. (2008). A sensitive flow cytometry-based nucleotide excision repair assay unexpectedly reveals that mitogen-activated protein kinase signaling does not regulate the removal of UV-induced DNA damage in human cells. J. Biol. Chem. *283*, 5533–5541.

Shevchenko, A., Wilm, M., Vorm, O., and Mann, M. (1996). Mass spectrometric sequencing of proteins silver-stained polyacrylamide gels. Anal. Chem. *68*, 850–858.

Shiohama, A., Sasaki, T., Noda, S., Minoshima, S., and Shimizu, N. (2003). Molecular cloning and expression analysis of a novel gene DGCR8 located in the DiGeorge syndrome chromosomal region. Biochem. Biophys. Res. Commun. *304*, 184–190.

Sohn, S.Y., Bae, W.J., Kim, J.J., Yeom, K.H., Kim, V.N., and Cho, Y. (2007). Crystal structure of human DGCR8 core. Nat. Struct. Mol. Biol. *14*, 847–853.

Swahari, V., Nakamura, A., Baran-Gale, J., Garcia, I., Crowther, A.J., Sons, R., Gershon, T.R., Hammond, S., Sethupathy, P., and Deshmukh, M. (2016). Essential Function of Dicer in Resolving DNA Damage in the Rapidly Dividing Cells of the Developing and Malignant Cerebellum. Cell Rep. *14*, 216–224.

Torrezan, G.T., Ferreira, E.N., Nakahata, A.M., Barros, B.D., Castro, M.T., Correa, B.R., Krepischi, A.C., Olivieri, E.H., Cunha, I.W., Tabori, U., et al. (2014). Recurrent somatic mutation in DROSHA induces microRNA profile changes in Wilms tumour. Nat. Commun. *5*, 4039.

Wada, T., Kikuchi, J., and Furukawa, Y. (2012). Histone deacetylase 1 enhances microRNA processing via deacetylation of DGCR8. EMBO Rep. *13*, 142–149.

Wallace, N.A., Robinson, K., Howie, H.L., and Galloway, D.A. (2012). HPV 5 and 8 E6 abrogate ATR activity resulting in increased persistence of UVB induced DNA damage. PLoS Pathog. *8*, e1002807.

Wang, Y., and Taniguchi, T. (2013). MicroRNAs and DNA damage response: implications for cancer therapy. Cell Cycle *12*, 32–42.

Wang, Y., Medvid, R., Melton, C., Jaenisch, R., and Blelloch, R. (2007). DGCR8 is essential for microRNA biogenesis and silencing of embryonic stem cell self-renewal. Nat. Genet. *39*, 380–385.

Wang, Y., Huang, J.W., Li, M., Cavenee, W.K., Mitchell, P.S., Zhou, X., Tewari, M., Furnari, F.B., and Taniguchi, T. (2011). MicroRNA-138 modulates DNA damage response by repressing histone H2AX expression. Mol. Cancer Res. *9*, 1100–1111.

Wei, W., Ba, Z., Gao, M., Wu, Y., Ma, Y., Amiard, S., White, C.I., Rendtlew Danielsen, J.M., Yang, Y.G., and Qi, Y. (2012). A role for small RNAs in DNA double-strand break repair. Cell *149*, 101–112.

Weitz, S.H., Gong, M., Barr, I., Weiss, S., and Guo, F. (2014). Processing of microRNA primary transcripts requires heme in mammalian cells. Proc. Natl. Acad. Sci. USA *111*, 1861–1866.

Yasuda, G., Nishi, R., Watanabe, E., Mori, T., Iwai, S., Orioli, D., Stefanini, M., Hanaoka, F., and Sugasawa, K. (2007). In vivo destabilization and functional defects of the xeroderma pigmentosum C protein caused by a pathogenic missense mutation. Mol. Cell. Biol. *27*, 6606–6614.

Yeom, K.H., Lee, Y., Han, J., Suh, M.R., and Kim, V.N. (2006). Characterization of DGCR8/Pasha, the essential cofactor for Drosha in primary miRNA processing. Nucleic Acids Res. *34*, 4622–4629.

Yi, R., Pasolli, H.A., Landthaler, M., Hafner, M., Ojo, T., Sheridan, R., Sander, C., O'Carroll, D., Stoffel, M., Tuschl, T., and Fuchs, E. (2009). DGCR8-dependent microRNA biogenesis is essential for skin development. Proc. Natl. Acad. Sci. USA *106*, 498–502.

Zhou, Y., Wang, J., Lu, X., Song, X., Ye, Y., Zhou, J., Ying, B., and Wang, L. (2013). Evaluation of six SNPs of MicroRNA machinery genes and risk of schizophrenia. J. Mol. Neurosci. *49*, 594–599.

Cell Reports, Volume *19*

Supplemental Information

DGCR8 Mediates Repair of UV-Induced DNA Damage Independently of RNA Processing

Philamer C. Calses, Kiranjit K. Dhillon, Nyka Tucker, Yong Chi, Jen-wei Huang, Masaoki Kawasumi, Paul Nghiem, Yemin Wang, Bruce E. Clurman, Celine Jacquemont, Philip R. Gafken, Kaoru Sugasawa, Masafumi Saijo, and Toshiyasu Taniguchi

SUPPLEMENTARY EXPERIMENTAL PROCEDURES

Antibodies and chemical inhibitors and activators

Rabbit polyclonal antibodies against human (5626) and murine (8889) phosho-S153 DGCR8 were generated by PhosphoSolutions. DGCR8 (10996-1-AP, Proteintech), DROSHA (Cell signaling), DICER (ab14601, Abcam), ERCC8 (15921-1-AP, Proteintech), FLAG (F1804, Sigma-Aldrich), phospho-H2A.X (05-636, Millipore), H2AX (05-636, Millipore), CSB (sc-25370, Santa Cruz Bio.), XPA (sc-853, Santa Cruz Bio.), XPC (A301-122A, Bethyl Lab.), vinculin (V9131, Sigma-Aldrich), RNA polymerase II H5 (MMS-129R, Covance), Pol II (N-20) (sc-899, Santa Cruz Biotechnology), CDK9 (C12F7) (2316, Cell signaling), phosphoP38 (2339, Cell signaling), CPD (CAC-NM-DND-001, Cosmo Bio Co.), 6-4PP (CAC-NM-DND-002, Cosmo Bio Co.), phospho-c-Jun (9261, Cell Signaling), phospho-JNK (4668, Cell Signaling) and JNK (9252, Cell Signaling) antibodies were used. SP600125 (JNK inhibitor) and anisomycin (JNK activator) were purchased from Tocris.

Recovery of RNA synthesis (RRS) assay

Coverslips were mounted on slides with Vectashield (Vector Laboratories). Image acquisitions were made with a TE2000 Nikon microscope with a 20x immersion objective, a CCD camera (CoolSNAP ES) and MetaVue software (Universal Imaging). EU signal intensity was measured by Cellomics software (Thermo Scientific). Cells without EU incubation were used as a negative control to subtract background signal.

siRNA and shRNA

siDGCR8 (5'-CCUUCAACUUCUACGGAGCUUC-3'),
siDrosha-1 (5'-AACGAGUAGGC UUCGUGACUU-3'),
siDrosha-2 (5'-AAGUCACGAAGCCUACUCG-3') and
siCSB (5'-CAGGACUCGUGGUUCAAAUUA-3') were used.
Lentiviral constructs containing shRNAs for DGCR8 (shRNA1: TRCN0000166035, shRNA2: TRCN0000165324, shRNA3: TRCN0000162331), Drosha (shRNA1: TRCN0000022249, shRNA2: TRCN0000022250), or XPC (shRNA1: TRCN0000083119, shRNA2: TRCN0000083118) were purchased from Sigma.

Mass spectrometry

In-line de-salting was accomplished using a reversed-phase trap column (100 μm × 20 mm) packed with Magic C_{18}AQ (5-μm 200Å resin; Michrom Bioresources, Auburn, CA) followed by peptide separations on a reversed-phase column (75 μm × 250 mm) packed with Magic C_{18}AQ (5-μm 100Å resin; Michrom Bioresources, Auburn, CA) directly mounted on the electrospray ion source. Chromatographic separations were conducted at a flowrate of 300 nL/min with a elution profile from 2%B to 2%B in 5 min, 2%B to 10%B in 3 min, 10%B to 40%B in 60 min, 40%B to 80%B in 2 min, and 80%B to 80%B in 10 min using 0.1% formic acid in water (a) and 0.1% formic acid in acetonitrile (b) as solvents. Data were collected in a data-dependent mode in which a high mass resolution/high mass accuracy scan (in the FT part of the instrument) was followed by low resolution/low mass accuracy MS/MS scans of the five most abundant ions from the preceding MS scan (in the LTQ part of the instrument). The FT part of the instrument

was set at a target resolution of 60,000 at m/z 400, an AGC target value of 1e6, and a maximum ion time of 150 ms while the ion trap was set to a MSn AGC target value of 1e4 and a MSn maximum ion time of 50 ms. The data-dependent method triggered a MS3 (MS/MS/MS) analysis on an MS2 (MS/MS) ion species if an MS2 ion species differed from the precursor ion species by m/z 98.0, 49.0, or 32.7, the neutral loss of phosphoric acid for a singly-, doubly-, or triply-charged ion species, respectively. Normalized collision energy of 35% and isolation widths of 2.0 were used for both MS2 and MS3 events. Dynamic exclusion was enabled with a repeat count of 1, a repeat duration of 15 seconds, an exclusion duration of 15 seconds, a low exclusion mass width of 0.55 and a high exclusion mass width of 1.55.
Raw MS/MS data were submitted to the Computational Proteomics Analysis System (CPAS) (Rauch et al., 2006) and searched using the X! Tandem search engine(Craig and Beavis, 2004) against the IPI human protein database (v3.59). Cys -17.027 Da, Glu -18.011 Da, Met +15.995, Gln -17.027, Ser +79.966, Thr +79.966, and Try +79.966 were set as variable modifications. The mass tolerances were set ±2 Da and ±0.5 Da for precursor and fragment ions, respectively. The enzyme was set to Trypsin, and up to 2 missed cleavages were permitted. Peptide validation was conducted with Peptide Prophet (Keller et al., 2002) and peptide identification results were filtered with false discovery rate of less than 5%.

Subcellular fractionation and immunoprecipitation

Subcellular fractionation was performed using a published protocol (Rockstroh et al., 2011). For λ phosphatase treatment, cells were lysed with lysis buffer (50nM Tris pH 7.4, 150nM NaCl, 1% Triton-X100, protease inhibitor (04693116011, Roche) on ice for 15 minutes. After centrifugation at 4 °C at 13.2K rpm for 15minutes, the supernatant was collected and incubated with 100 units of λ phosphatase supplemented with 1mM $MnCl_2$ (P0753, New England BioLabs) and with or without phosphatase inhibitors (50mM NaF and 10mM $NaVO_4$). After incubation for 1 hour at 30 °C, samples were boiled in sample buffer for 5 minutes. For the immunoprecipitation, cells were lysed with lysis buffer (20mM Tris-HCl pH 7.4, 150mM NaCl, 0.5% NP40, 2mM $MgCl_2$, 125units/mL Universal Nuclease (88702, Thermo Scientific) on ice for 30 minutes. After centrifugation at 4 °C at 13.2K rpm for 5 minutes, the supernatant was collected. One mg of protein lysate was pre-cleared in lysis buffer with protein A/G Plus-Agarose (sc-2003, Santa Cruz Biotechnology) incubated for 30 minutes at 4 °C on a shaker. After centrifugation at 4 °C at 2K rpm for 5 minutes, 2 μg of anti-FLAG antibody (F1804, Sigma-Aldrich) or normal mouse IgG (sc-2025, Santa Cruz Biotechnology) was added in the pre-cleared protein lysates. After an overnight incubation at 4 °C on a shaker, protein A/G Plus-Agarose was added into the mix and incubated at 4 °C on a shaker for 2 hours. Then, the lysates were washed 3 times with lysis buffer. After the last wash, lysates were boiled at 95°C in sample buffer. To detect DGCR8, RNAPII and CSB interaction, cells were cross-linked in 1% para-formaldehyde for 10 minutes at room temperature, then quenched with 125mM glycine for 5 minutes at room temperature before proceeding with immunoprecipitation as described above. Then, the immunoprecipitated samples were boiled at 95°C in sample buffer for 10 minutes to reverse the cross-links. The western blot was done as described above. To detect the UV-induced DGCR8 upward shift shown in **Figure 1a, 1b, and 1e**, large 7.5% SDS-PAGE gels were used.

Chemiluminescence was used for detection, and membranes were digitally scanned by Imagequant LAS 4000 (GE Biosciences).

Micropore UV irradiation

To determine whether pS153-DGCR8 was localized at UV-induced CPDs, cells were plated onto coverslips, covered with a 5 μm micropore filter (TMTP01300, Millipore) and treated with 100 J/m^2 UVC. After one hour, cells were fixed and permeabilized as described above. Then, cells were treated with 2M HCl to denature DNA for 30 minutes at room temperature. After several washes with washing buffer, cells were blocked with 3% BSA in PBS for 20 minutes at room temperature and then incubated with anti-CPDs and anti-pS153 DGCR8 overnight at 4 °C. After several washes with washing buffer, cells were incubated for one hour at room temperature with Alexa-fluor 488 goat anti-rabbit (A11034, Life Technologies) and Alexa-fluor 594 donkey anti-mouse (A21203, Life Technologies) secondary antibodies. Subsequent steps were done as described in the main text under immunofluorescent microscopy in the material and methods section.

MicroRNA profiling

Differential Expression: Raw Ct values were generated for four biological replicates. Samples were from two batches (two replicates per batch). MiRNAs with Ct values available for at least 3 replicates were analyzed for differential expression (117 miRNAs out of 257 non-control miRNAs) (n = 4 for 86 miRNAs, n = 3 for 31 miRNAs). SNORD38b snoRNA was used as an internal control. Ct values of SNORD38b snoRNA were subtracted from all raw Ct values for the 117 miRNAs respectively for each sample, per replicate, to obtain ΔCt values. Mean ΔCt values from at least 3 biological replicates were used to carry out pairwise ΔΔCt calculation using either mean ΔCt from control untreated or mean ΔCt from control UV-treated cells as basis for comparison. ΔΔCt values were log transformed. Heatmaps were generated in R using the 'gplots' package. Statistical Testing: ΔCt values (from at least 3 biological replicates) were log transformed prior to pairwise statistical testing with Student's t-test. MiRNAs with $p < 0.05$ were considered to be statistically significantly differentially expressed. Relative expression was calculated for individual miRNAs with statistically significant differential expression in DGCR8-depleted cells relative to control or DGCR8-depleted cells complimented with wildtype DGCR8, untreated and 24 hours after 20J/m^2 UVC treatment. ΔCt values of control or control +UVC were used as a baseline for pairwise comparison across 3 to 4 biological replicates. Relative expression was calculated by taking the inverse mean ΔCt relative to control or control +UVC across replicates.

Cited References

Craig, R., and Beavis, R.C. (2004). TANDEM: matching proteins with tandem mass spectra. Bioinformatics *20*, 1466-1467.

Keller, A., Nesvizhskii, A.I., Kolker, E., and Aebersold, R. (2002). Empirical statistical model to estimate the accuracy of peptide identifications made by MS/MS and database search. Analytical chemistry *74*, 5383-5392.

Rauch, A., Bellew, M., Eng, J., Fitzgibbon, M., Holzman, T., Hussey, P., Igra, M., Maclean, B., Lin, C.W., Detter, A., et al. (2006). Computational Proteomics Analysis

System (CPAS): an extensible, open-source analytic system for evaluating and publishing proteomic data and high throughput biological experiments. Journal of proteome research *5*, 112-121.
Rockstroh, M., Müller, S.A., Jende, C., Kerzhner, A., von Bergen, M., and M. Tomm, J.M. (2011). Cell fractionation - an important tool for compartment proteomics. Journal of Integrated OMICS *1*, 135-143.

Figure S1, Calses et al.

A

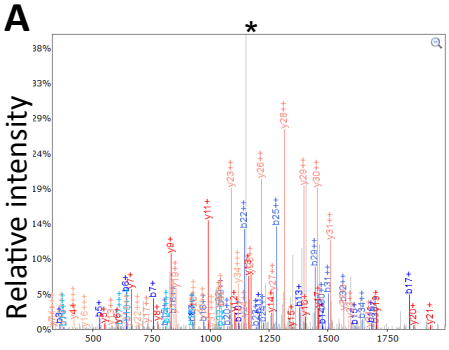

B

b+	b2+	b3+	#	Seq	#	y+	y2+	y3+
72.0444	36.5258	24.6863	1	A	36			
201.0870	101.0471	67.7005	2	E	35	3480.5448	1740.7760	1160.8531
361.1177	181.0625	121.0441	3	C	34	3351.5022	1676.2547	1117.8389
418.1391	209.5732	140.0512	4	G	33	3191.4715	1596.2394	1064.4953
531.2232	266.1152	177.7459	5	L	32	3134.4500	1567.7287	1045.4882
644.3073	322.6573	215.4406	6	L	31	3021.3660	1511.1866	1007.7935
757.3913	379.1993	253.1353	7	L	30	2908.2819	1454.6446	970.0988
924.3897	462.6985	308.8014	8	S	29	2795.1978	1398.1026	932.4041
1021.4424	511.2248	341.1523	9	P	28	2628.1995	1314.6034	876.7380
1120.5108	560.7591	374.1751	10	V	27	2531.1467	1266.0770	844.3871
1207.5429	604.2751	403.1858	11	S	26	2432.0783	1216.5428	811.3643
1264.5643	632.7858	422.1930	12	G	25	2345.0463	1173.0268	782.3536
1379.5913	690.2993	460.5353	13	D	24	2288.0248	1144.5161	763.3465
1478.6597	739.8335	493.5581	14	V	23	2172.9979	1087.0026	725.0041
1615.7186	808.3629	539.2444	15	H	22	2073.9295	1037.4684	691.9813
1686.7557	843.8815	562.9234	16	A	21	1936.8706	968.9389	646.2950
1846.7864	923.8968	616.2670	17	C	20	1865.8335	933.4204	622.6160
1943.8392	972.4232	648.6179	18	P	19	1705.8028	853.4050	569.2724
2090.9076	1045.9574	697.6407	19	F	18	1608.7500	804.8786	536.9215
2147.9290	1074.4682	716.6479	20	G	17	1461.6816	731.3444	487.8987
2204.9505	1102.9789	735.6550	21	G	16	1404.6601	702.8337	468.8916
2291.9825	1146.4949	764.6657	22	S	15	1347.6387	674.3230	449.8844
2391.0509	1196.0291	797.6885	23	V	14	1260.6066	630.8070	420.8737
2448.0724	1224.5398	816.6957	24	G	13	1161.5382	581.2727	387.8509
2563.0993	1282.0533	855.0380	25	D	12	1104.5168	552.7620	368.8438
2620.1208	1310.5640	874.0451	26	G	11	989.4898	495.2485	330.5015
2719.1892	1360.0982	907.0679	27	V	10	932.4684	466.7378	311.4943
2776.2107	1388.6090	926.0751	28	G	9	833.3999	417.2036	278.4715
2889.2947	1445.1510	963.7698	29	I	8	776.3785	388.6929	259.4643
2946.3162	1473.6617	982.7769	30	G	7	663.2944	332.1508	221.7697
3003.3377	1502.1725	1001.7841	31	G	6	606.2729	303.6401	202.7625
3132.3803	1566.6938	1044.7983	32	E	5	549.2515	275.1294	183.7553
3219.4123	1610.2098	1073.8089	33	S	4	420.2089	210.6081	140.7411
3290.4494	1645.7283	1097.4880	34	A	3	333.1769	167.0921	111.7305
3405.4764	1703.2418	1135.8303	35	D	2	262.1397	131.5735	88.0514
			36	K	1	147.1128	74.0600	49.7091

C

```
DGCR8_ Homo sapiens(Human)                  TGAERDVRAECGLLLSPVSGDVHACP
DGCR8_ Macaca mulatta(Rhesus macaque)       TGAERDVRAECGLLLSPVIGDVHACP
DGCR8_ Felis catus(Cat)                     TGVERDARADCGLALSPVSGDVHACP
DGCR8_ Equus caballus(Horse)                TGVERDARAECGRALSPVSGDVHACP
DGCR8_ Cavia porcellus(Guinea pig)          TGVEHDTRAECSLLLSPLSGDMHACP
DGCR8_ Oryctolagus cuniculus(Rabbit)        TGAERDARAECGPLPSPGSGDVHACP
DGCR8_ Canis familiaris(Dog)                TGVERDARAECGLALSPVSGDVHACP
DGCR8_ Sus scrofa(Pig)                      TGAERDARAECTLALSPVSGDVHACP
DGCR8_ Ovis aries(Sheep)                    TGAERDVRAECGLALSPVSGDVHAGP
DGCR8_ Gallus gallus(Chicken)               TGIEQDYKADTDFGINNVNGDLHVCP
DGCR8_ Danio rerio(Zebrafish)               TGFGQVSDE--DQSLESINGELHDSV
DGCR8_ Xenopus laevis(African clawed frog)  TGLECEGSLHGGSNMNSVNGDMYVCP
X777_16613_ Cerapachys biroi(Ant)           GTALVN--------QSSTSDDSHCHE
```

D

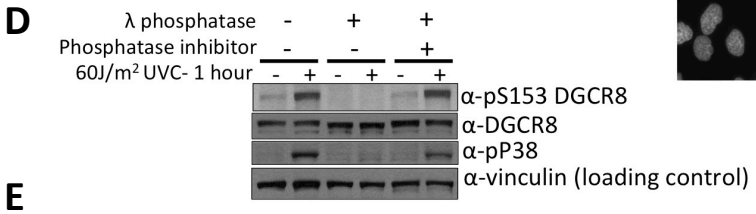

E

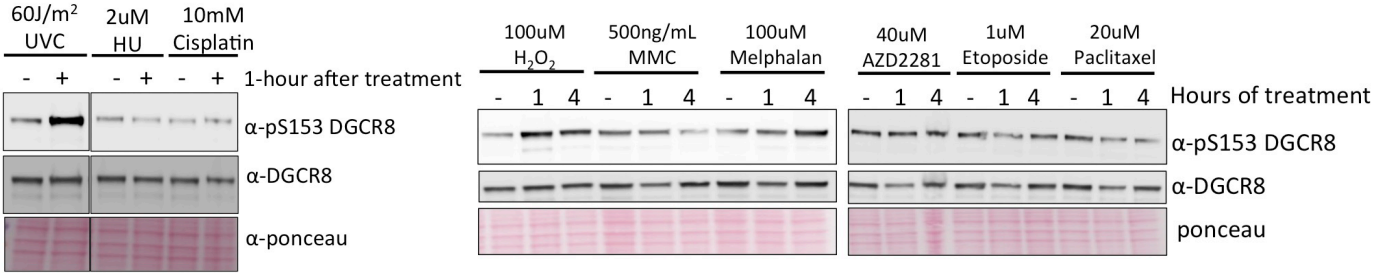

F

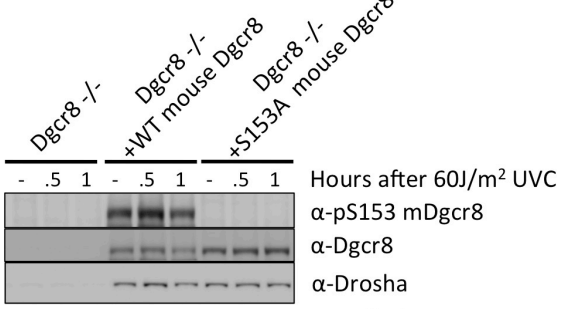

G

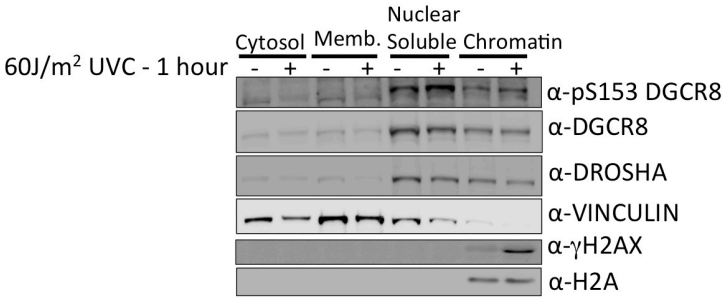

H

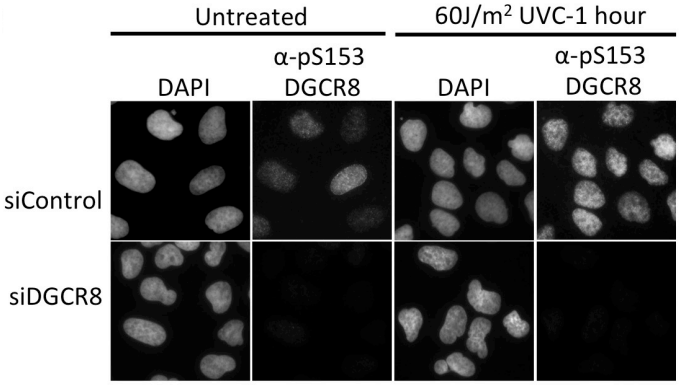

I

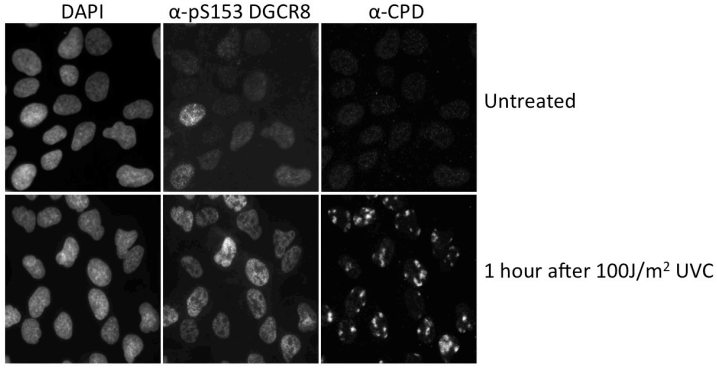

Figure S1. S153 of DGCR8 is phosphorylated in response to UV, Related to Figure 1.

(A) Phosphosite identification of S153 in DGCR8**.** A gel band of DGCR8 subjected to UV light exposure was proteolytically digested with trypsin and subjected to tandem mass spectrometry as described in "Methods and Materials". A triply charged monoisotopic ion m/z 1184.5325 was selected for tandem mass spectrometry and the resulting spectrum is displayed. The "*" in the spectrum labels a peak corresponding to the neutral loss of m/z 32.7 from the precursor ion equaling the loss of H_3PO_4, which is a common occurrence during the tandem mass analysis of phosphopeptides. (B) The tandem mass spectrum from panel A was subjected to phosphopeptide identification using the database search algorithm X!Tandem. The algorithm identified the peptide A146 to K181 containing a single phosphate group located to S153 as shown (highlighted in yellow). The panel displays all predicted fragment ions for the identified peptide and highlights in red and blue the y-ions and b-ions, respectively, that were identified in the tandem mass spectrum in panel A. The m/z difference between the predicted triply-charged ion species (m/z 1184.5321) for singly phosphorylated A146 to K181 peptide and the measured triply-charged ion species (m/z 1184.5325) is 0.0004. (C) DGCR8 S153 sequence alignment. S153 is conserved among mammals, but not in other eukaryotes. (D) Immunoblot. U2OS cells depleted of DGCR8 were corrected with FLAG-WT DGCR8, and treated with UVC (60 J/m^2). Cell lysates were treated with λ phosphatase +/- phosphatase inhibitors. S153 phosphorylation was induced after UV treatment. Treatment with λ phosphatase led to elimination of phosphoS153 signal. Co-treatment with phosphatase inhibitors restored phosphoS153 signal. (E) Immunoblot. U2OS cells were treated with several DNA damaging agents and cellular stressors. (F) Immunoblot. Indicated mouse embryonic fibroblasts were irradiated with +/-UV and harvested at the indicated time points. (G) Immunoblot. U2OS cells untreated or treated with UVC were subjected to subcellular fractionation followed by western blotting. (H) Immunocytochemistry. U2OS cells transfected with indicated siRNAs were +/-UVC irradiated and subjected to immunocytochemistry with phospho-S153 DGCR8 antibody. Phospho-S153 signal was detected in the nuclei in control siRNA-transfected cells (but not in DGCR8-siRNA transfected cells). PhosphoS153 signal was detected in some untreated cells, but the signal was greatly increased after UV treatment. (I) Micropore UV irradiation and immunofluorescent microscopy. U2OS cells were UVC irradiated at 100 J/m^2 through a micropore filter (5 μm pore diameter). At 1 hour after UVC exposure, cells were double immunostained with anti-phosphoS153-DGCR8 and anti-CPD antibodies. Even with localized UV irradiation, phosphoS153-DGCR8 signal was induced diffusely in the nuclei.

Figure S2, Calses et al.

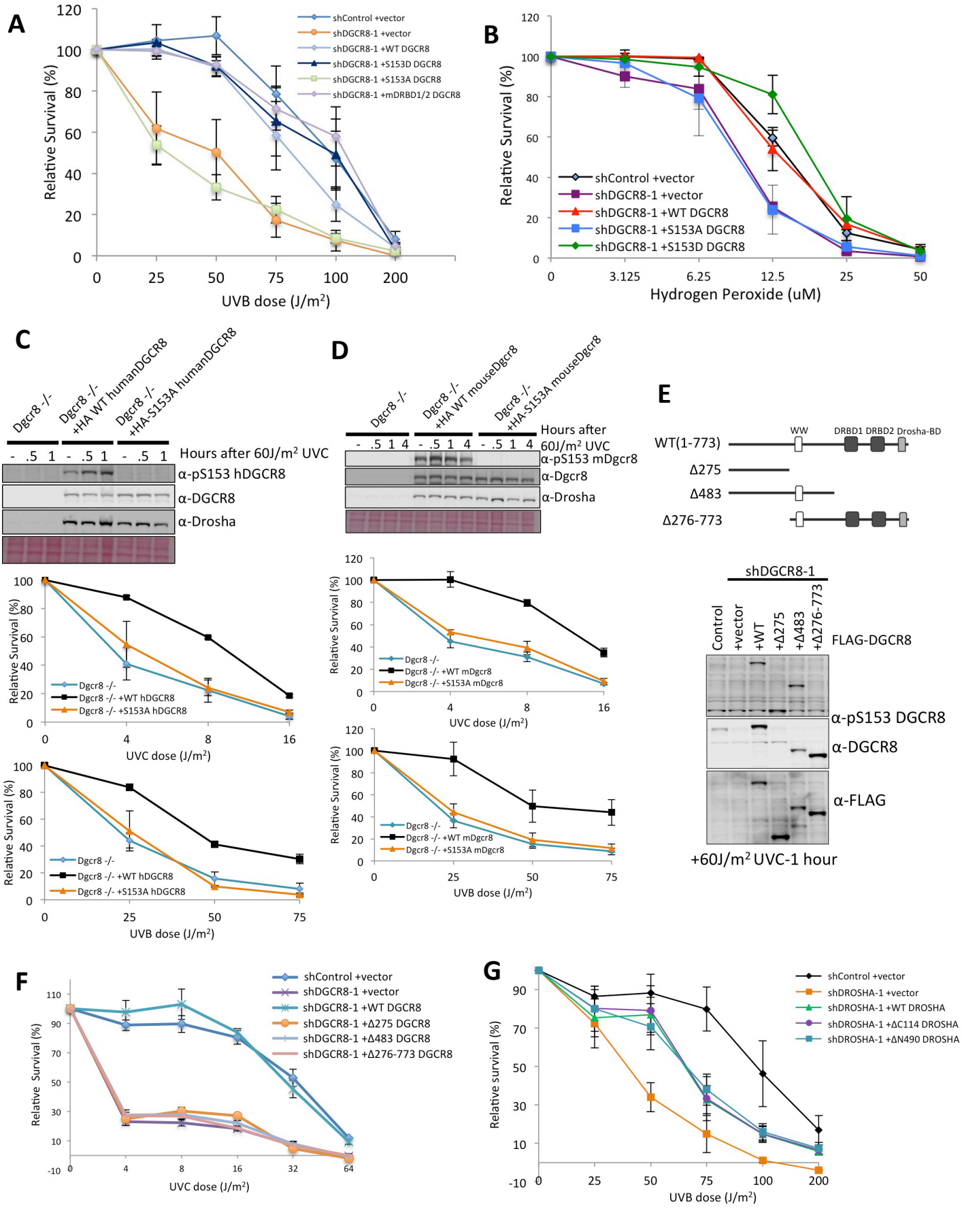

Figure S2. DGCR8 and Drosha are critical for cellular resistance to UV, Related to Figure 2 and Figure 3.

(A) UVB sensitivity assay of DGCR8-depleted HCT116 cells transduced with the indicated DGCR8 constructs. (B) Hydrogen peroxide sensitivity assay of DGCR8-depleted HCT116 cells transduced with the indicated DGCR8 constructs. (C, D) Immunoblot and UV sensitivity assay. Dgcr8 knockout mouse embryonic fibroblasts were transduced with HA-tagged human DGCR8 (wild type or S153A mutant) or HA-tagged mouse Dgcr8 (wild type or S153A mutant). These cells were irradiated with +/- UV, harvested at the indicated time points and subjected to immunoblot. UVC and UVB sensitivities of these cells were also tested. (E) Schematic presentation of DGCR8 deletion mutants. Immunoblot shows expression of the indicated shRNA-resistant DGCR8 deletion mutants and wild-type DGCR8 in DGCR8-depleted HCT116 cells. The DGCR8 antibody does not detect Δ275-DGCR8. (F) UVC sensitivity assay. DGCR8-depleted HCT116 cells were transduced with the indicated DGCR8 constructs and plated for survival after +/-UV treatment. (G) Drosha is critical for cellular resistance to UVB. Drosha depletion led to hypersensitivity to UVB in HCT116 cells. Reintroduction of shRNA-resistant wild-type, ΔC114 (RNA binding domain mutant, microRNA processing deficient) or ΔN490 (DGCR8 binding deficient, microRNA processing deficient) Drosha restored UVB resistance in Drosha-depleted HCT116 cells. All UV sensitivity data represent mean values +/- SEM of three independent experiments.

FigureS3, Calses et al.

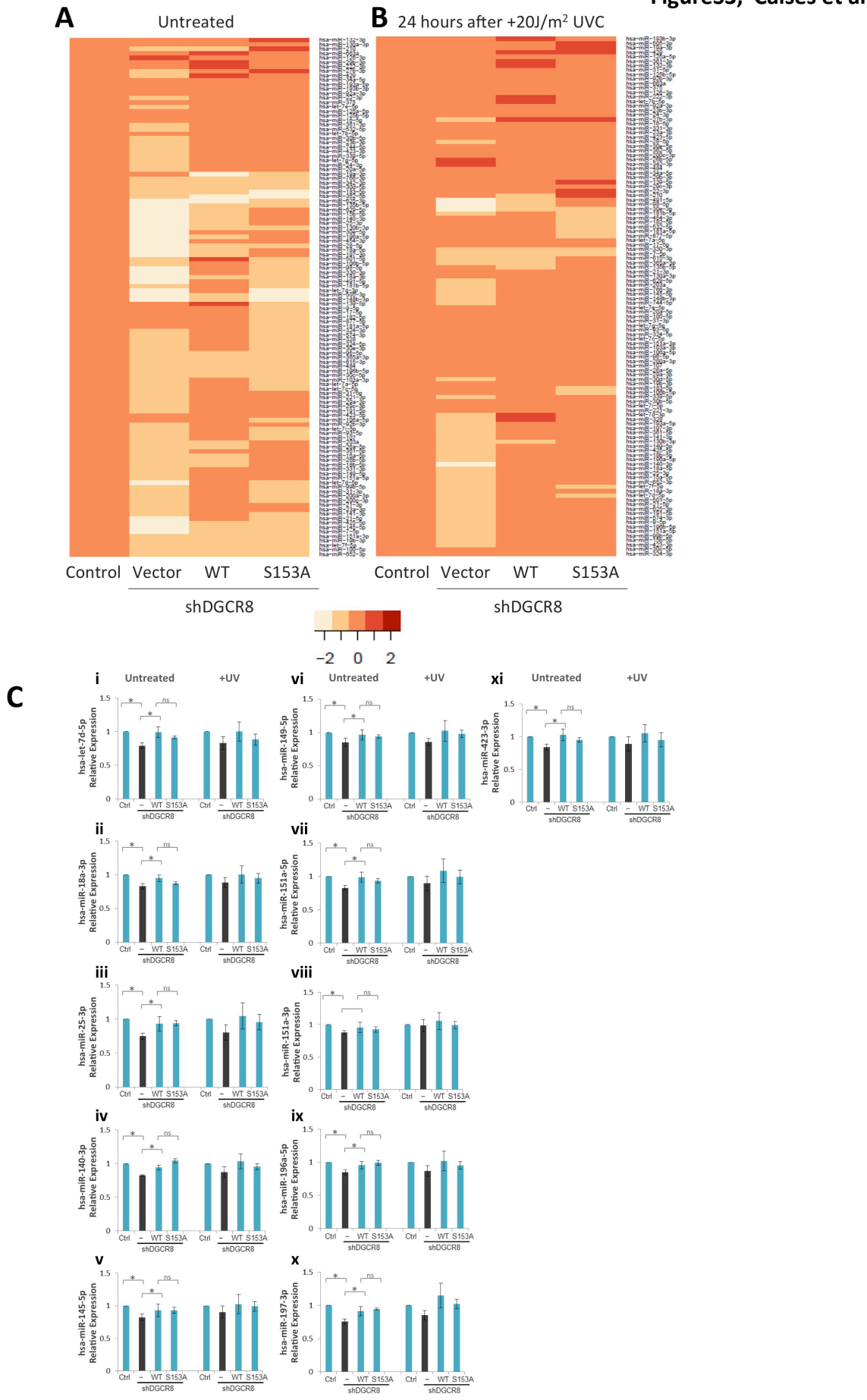

Figure S3. Phosphorylation of S153 of DGCR8 is not critical for miRNA expression, Related to Figure 2.

(A) Heatmaps of differential expression of DGCR8-dependent miRNAs. Downregulation of a subset of miRNAs that occurred upon DGCR8 depletion was rescued by expression of either wildtype or DGCR8 153A mutant protein in DGCR8-depleted HCT116 cells. Expression of miRNA's identified to have statistically different expression in untreated DGCR8-depleted cells (+Vector) relative to untreated control cells is shown. For (A) untreated control and DGCR8-depleted cells expressing empty vector, wild-type DGCR8, or DGCR8 153A-mutant and for (B), UV-treated control and DGCR8- depleted cells expressing empty vector, wild-type DGCR8, or DGCR8 153A-mutant are shown. Decreased expression is indicated in shades of lighter shades of orange/red, while increased relative expression is indicated in darker shades of red. Clustering by rows (miRNAs) has been applied to heatmaps for better visualization. The values were normalized so that those of control cells transduced with empty vector are set to zero. (C) (panels i – xi) Relative expression is shown for miRNAs with statistically significant differential expression in DGCR8-depleted cells relative to control or DGCR8-depleted cells complemented with wildtype DGCR8, untreated and 24 hours after $20J/m^2$ UVC . Relative expression shown is the inverse mean of ΔCt values relative to control across 3 to 4 replicates. Error bars indicate SEM across biological replicates. An "*" indicates statistically significant differential expression ($p < 0.05$) and an "ns" indicates a non-significant result. None of the UV treated samples showed statistically significant results.

Figure S4, Calses et al.

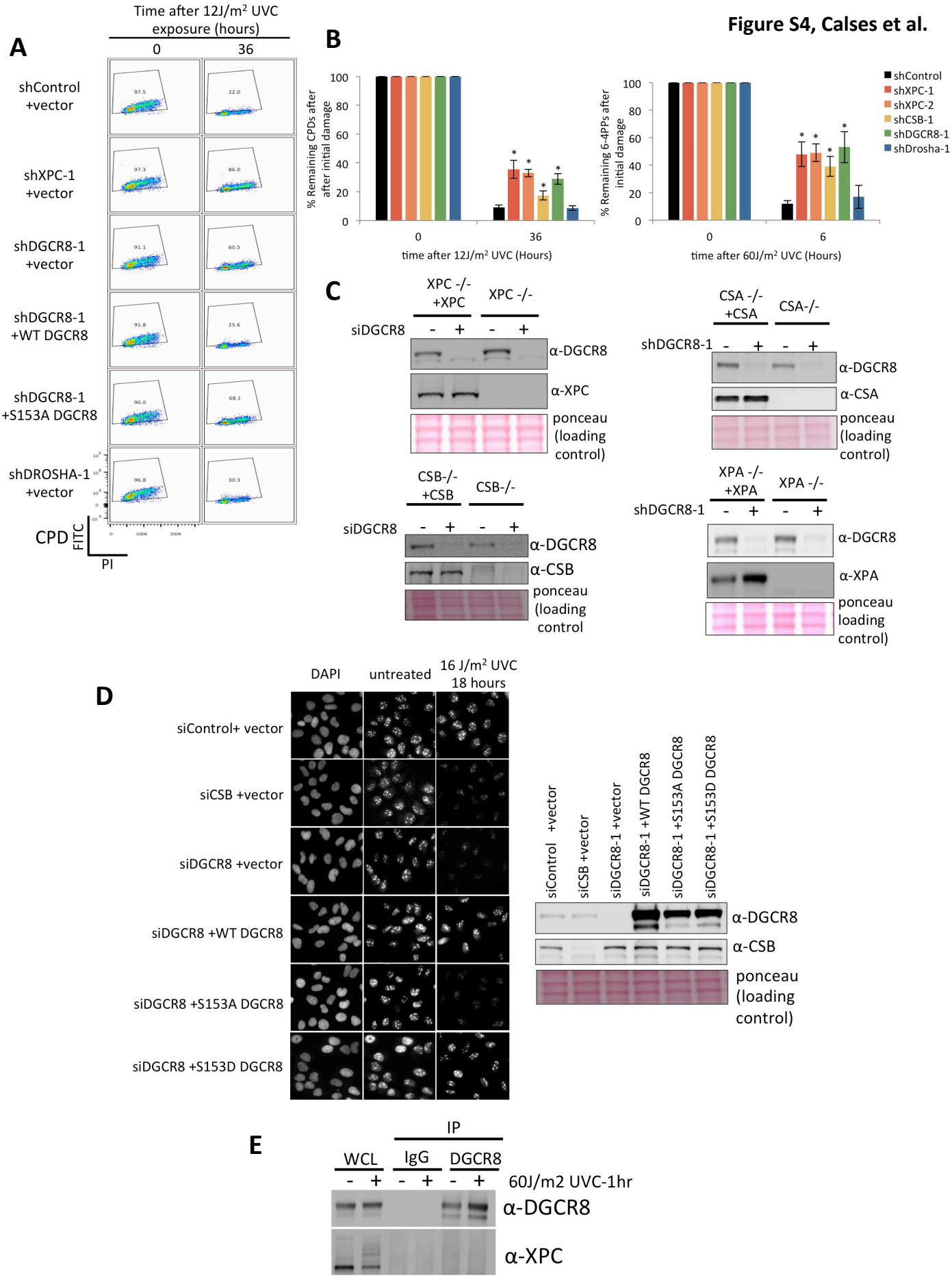

Figure S4. Phosphorylation of S153 of DGCR8 is required for efficient transcription-coupled nucleotide excision repair, Related to Figure 4 and Figure 5. (A) Representative images for experiments shown in Figure 4A. Removal of CPDs assessed by flow cytometry using anti-CPD antibody. HCT116 cells depleted of indicated genes, and complemented with indicated constructs were treated with UVC, and CPD positive cells at the indicated time points were measured using flow cytometry. (B) Removal of CPDs or 6-4PPs assessed by flow cytometry using anti-CPD and anti-6-4PP antibodies. HCT116 cells depleted of indicated genes were treated with UVC, and CPD positive cells and 6-4PP positive cells at the indicated time points were measured. Asterisks indicate significant difference ($p<0.05$) relative to shControl +empty vector transduced cells. (C) Immunoblot. DGCR8 was depleted using siRNA or shRNA in XPC-, CSA-, CSB-, or XPA-deficient fibroblasts and their corrected counterparts. (D) Representative images for experiments shown in Figure 4C. Recovery of RNA synthesis (RRS) assay. Immunofluorescence images of 5' EU incorporation in U2OS cells before and after UVC radiation at 16J/m^2. U2OS cells transfected with indicated siRNAs and indicated cDNA constructs were subjected to the assay. Western blot confirmed depletion of CSB and DGCR8 by siRNAs and expression of the siRNA-resistant wild-type and mutant DGCR8 constructs. (E) IP-western. Cell lysate of UV-treated (or untreated) U2OS cells transduced with a wild type DGCR8 construct were immunoprecipitated with the indicated antibodies. Immunoblot was done using the indicated antibodies.

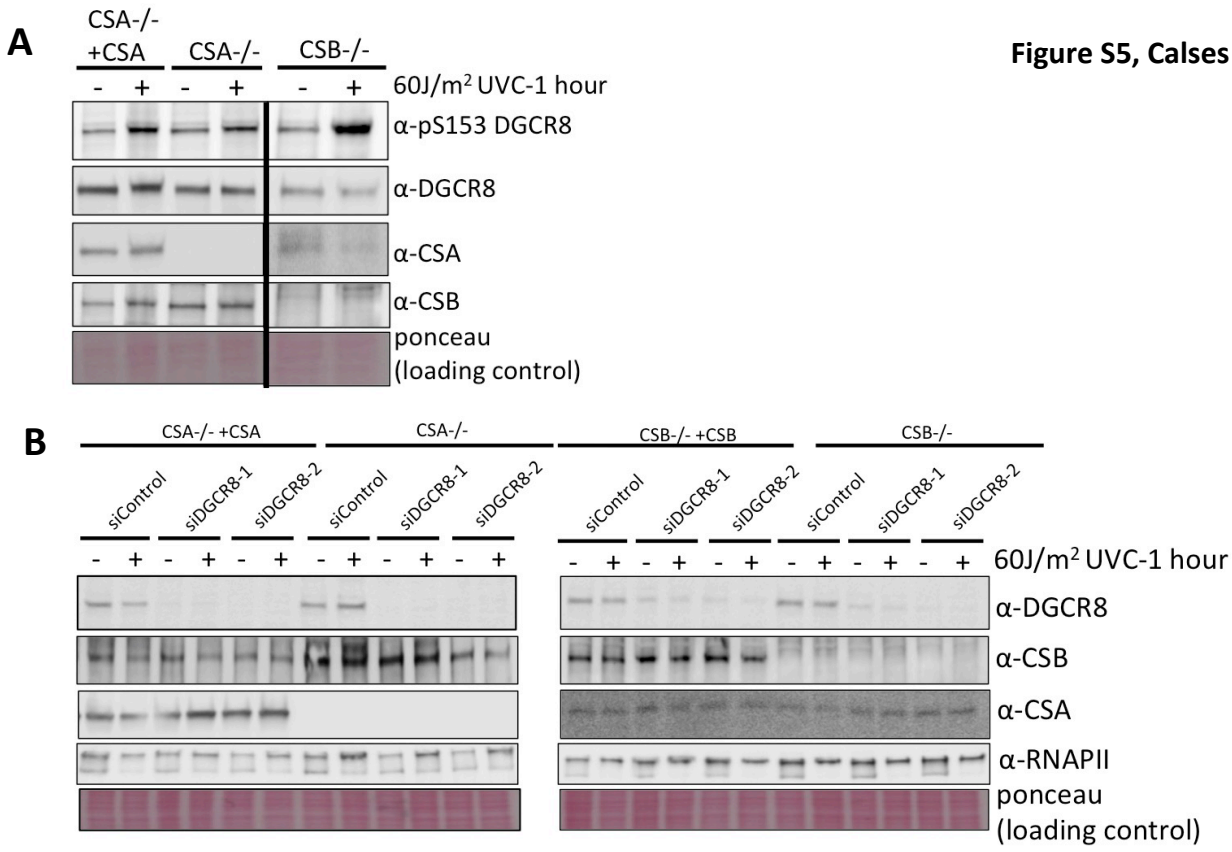

Figure S5, Calses et al.

Figure S5. UV-induced S153 phosphorylation on DGCR8 in not downstream of CSB or CSA, Related to Figure 5. (A) Immunoblot. CSA-, or CSB -deficient fibroblasts and their corrected counterparts were subjected to immunoblot. CSA or CSB deficiency did not affect UV-induced phosphorylation of S153 of DGCR8 (B) DGCR8 was depleted using siRNA in CSA-, or CSB-deficient fibroblasts and their corrected counterparts. DGCR8 depletion did not affect expression of CSA, CSB, or RNAPII.

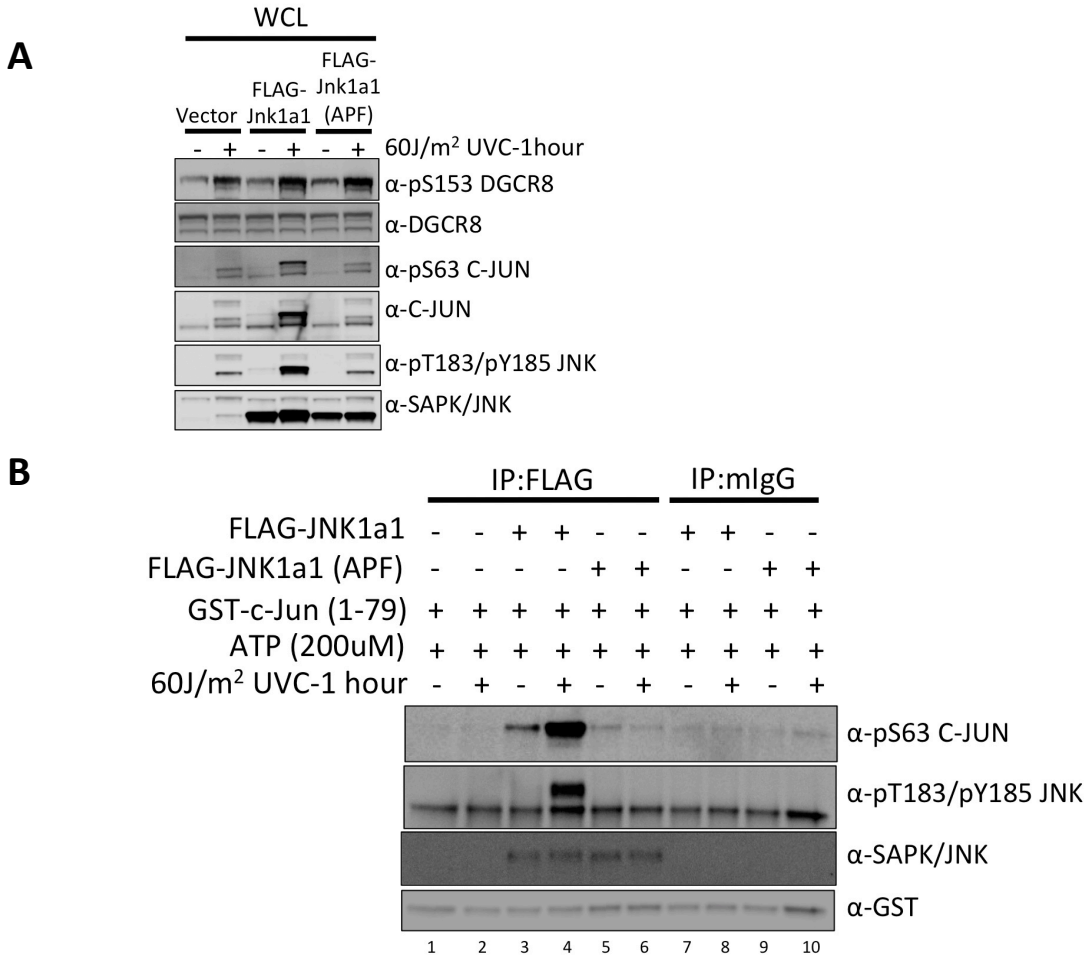

Figure S6. JNKs are involved in phosphorylation of S153 on DGCR8, Related to Figure 6. (A) Immunoblot. Whole cell lysate (WCL) from U2OS cells transfected with vector, WT-JNK or kinase-dead-JNK (APF) used for in vitro kinase assay shown in Figure6D-E. (B) Immunoblot after *in vitro* kinase assay. Recombinant GST-tagged human C-JUN (aa1-79) fragment was used as a substrate and immunopurified WT JNK1a1 or kinase-dead JNK1a1 (APF) was used as the enzyme in the *in vitro* kinase assay.